NASA TECHNICAL NOTE

NASA TN D-7183

NASA TN D-7183

LOW-SPEED WIND-TUNNEL INVESTIGATION OF A SEMISPAN STOL JET TRANSPORT WING-BODY WITH AN UPPER-SURFACE BLOWN JET FLAP

by

Arthur E. Phelps

Langley Directorate
U.S. Army Air Mobility R&D Laboratory

and

William Letko and Robert L. Henderson

Langley Research Center
Hampton, Va. 23665

NATIONAL AERONAUTICS AND SPACE ADMINISTRATION • WASHINGTON, D. C. • MAY 1973

1. Report No.	2. Government Accession No.	3. Recipient's Catalog No.
NASA TN D-7183		

4. Title and Subtitle	5. Report Date
LOW-SPEED WIND-TUNNEL INVESTIGATION OF A SEMISPAN STOL JET TRANSPORT WING-BODY WITH AN UPPER-SURFACE BLOWN JET FLAP	May 1973
	6. Performing Organization Code
7. Author(s) Arthur E. Phelps, Langley Directorate, U.S. Army Air Mobility R&D Laboratory; William Letko and Robert L. Henderson, Langley Research Center	8. Performing Organization Report No. L-8740
	10. Work Unit No. 760-61-02-01
9. Performing Organization Name and Address NASA Langley Research Center Hampton, Va. 23665	11. Contract or Grant No.
	13. Type of Report and Period Covered Technical Note
12. Sponsoring Agency Name and Address National Aeronautics and Space Administration Washington, D.C. 20546	14. Sponsoring Agency Code

15. Supplementary Notes

16. Abstract

An investigation of the static longitudinal aerodynamic characteristics of a semispan STOL jet transport wing-body with an upper-surface blown jet flap for lift augmentation was conducted at the Langley Research Center in a low-speed wind tunnel having a 3.7-m (12-ft) octagonal test section. The semispan swept wing had an aspect ratio of 3.92 (7.84 for the full span) and had two simulated turbofan engines mounted ahead of and above the wing in a siamese pod equipped with an exhaust deflector. The purpose of the deflector was to spread the engine exhaust into a jet sheet attached to the upper surface of the wing so that it would turn downward over the flap and provide lift augmentation. The wing also had optional boundary-layer control provided by air blowing through a thin slot over a full-span plain trailing-edge flap.

17. Key Words (Suggested by Author(s))	18. Distribution Statement
STOL Jet flap Propulsive lift Upper-surface blowing Over-the-wing blowing	Unclassified – Unlimited

19. Security Classif. (of this report)	20. Security Classif. (of this page)	21. No. of Pages	22. Price*
Unclassified	Unclassified	41	$3.00

*For sale by the National Technical Information Service, Springfield, Virginia 22151

LOW-SPEED WIND-TUNNEL INVESTIGATION OF A SEMISPAN STOL JET TRANSPORT WING-BODY WITH AN UPPER-SURFACE BLOWN JET FLAP

By Arthur E. Phelps
Langley Directorate, U.S. Army Air Mobility R&D Laboratory

William Letko and Robert L. Henderson
Langley Research Center

SUMMARY

An investigation of the static longitudinal aerodynamic characteristics of a semispan STOL jet transport wing-body with an upper-surface blown jet flap for lift augmentation was conducted at the Langley Research Center in a low-speed wind tunnel having a 3.7-m (12-ft) octagonal test section. The semispan swept wing had an aspect ratio of 3.92 (7.84 for the full span) and had two simulated turbofan engines mounted ahead of and above the wing in a siamese pod equipped with an exhaust deflector. The purpose of the deflector was to spread the engine exhaust into a jet sheet attached to the upper surface of the wing so that it would turn downward over the flap and provide lift augmentation. The wing also had optional boundary-layer control provided by air blowing through a thin slot over a full-span plain trailing-edge flap.

The results of the investigation showed that very high lift coefficients could be achieved for STOL operations with the test configuration and that the performance was comparable to that of other powered-lift STOL concepts. The combination of engine exhaust deflectors and blowing boundary-layer control was found to be effective for maintaining flow attachment over the flaps for the entire operational envelope. The use of a plain flap behind the engines, which appears from previous work to have an advantage in reducing the noise level, resulted in lower diving moments than those associated with more complicated flap arrangements which have substantial rearward chord extension when deflected.

INTRODUCTION

With increasing population densities and economic pressures, interest in the development of short take-off and landing (STOL) jet transport aircraft has grown considerably. Several concepts have been proposed to meet the high lift demands of STOL operation, and

a wide variety of these have been tested. In most of the concepts under consideration, power is used for lift augmentation as well as for propulsion. Unfortunately, the large amount of energy required by propulsive-lift systems generally results in high noise. Recent unpublished preliminary noise studies have shown that one high-lift concept which shows promise for reducing the noise of STOL aircraft is that of an upper-surface blown jet flap (USB). The USB produces high lift by exhausting all of the jet engine efflux above the wing in such a manner that it becomes attached to the wing and turns downward over the flap. In suggested applications of this concept the jet efflux is usually flattened into a thin sheet by a specially designed nozzle. Essentially the USB relies upon the Coanda effect (ref. 1) to cause the exhaust of turbofan engines mounted on top of the wing to attach to the upper surface of the wing and the trailing-edge flap, thereby eliminating the noise which is normally associated with the impingement of the exhaust jet on the flaps and slots of a blown-flap system utilizing underslung engines. Also, in the upper-surface blowing arrangement the wing tends to shield the basic engine noise radiated below the aircraft. Additionally, this arrangement appears to offer structural and mechanical advantages over other jet-augmented high-lift concepts since a simple plain flap may be used.

The tests of reference 2, which were performed in the late 1950's, showed the USB to be effective in producing high lift with the thin high-pressure jets tested at that time but there was some question as to the effectiveness of the concept with modern high-bypass-ratio turbofan engines, which would result in a much thicker and lower pressure jet. Consequently, the present investigation was undertaken in order to provide some fundamental information on the aerodynamic characteristics of a swept wing model having dimensional features considered to be representative of STOL aircraft that might use high-bypass-ratio turbofan engines. This model utilized various engine exhaust deflectors mounted on top of the nacelle to flatten and spread the jet exhaust and incorporated optional boundary-layer control (BLC) at the knee of the trailing-edge flap.

The main body of the tests was conducted for two flap-deflection arrangements and one nacelle configuration which was selected on the basis of preliminary tests made to determine the effect of the various exhaust-deflector configurations. Tests were then made through an angle-of-attack range for several different values of thrust and flap-blowing momentum coefficients, and force and moment data were recorded at each angle of attack.

SYMBOLS

The data are referred to the stability-axis system shown in figure 1. The origin of the axes was located to correspond to a center-of-gravity position of 50 percent of the mean aerodynamic chord.

Values are given in both SI and U.S. Customary Units. The measurements and calculations were made in U.S. Customary Units.

A	aspect ratio, $b^2/2S$
S	area of semispan wing, m^2 (ft^2)
b	wing span (twice semispan), m (ft)
c_w	local wing chord, m (ft)
$\bar{c}$	mean aerodynamic chord, m (ft)
C_D	drag coefficient, D/qS
C_L	lift coefficient, L/qS
$C_{L,max}$	maximum lift coefficient
$C_{L,trim}$	lift coefficient with pitch trim supplied by a lift load on a tail $3.5\bar{c}$ aft of the c.g.
C_m	pitching-moment coefficient, $M_Y/qS\bar{c}$
C_μ	gross thrust coefficient of the engines (momentum coefficient of the jet efflux), T/qS
$C_{\mu,BLC}$	momentum coefficient of boundary-layer control system, $\dot{m}_{BLC}V_j/qS$
D	drag, N (lb)
F_A	axial force $(-F_X)$, N (lb)
F_N	normal force $(-F_Z)$, N (lb)
F_X	force directed along X-axis of model, N (lb)
F_Z	force directed along Z-axis of model, N (lb)
L	lift, N (lb)

$\dot{m}_{BLC}$	mass flow rate of boundary-layer-control air, kg/sec (slugs/sec)
M_Y	pitching moment, m-N (ft-lb)
q	free-stream dynamic pressure, N/m^2 (lb/ft^2)
R	Reynolds number based on $\bar{c}$
T	static thrust, N (lb)
V	free-stream velocity, m/sec (ft/sec)
V_j	velocity of boundary-layer-control jet, m/sec (ft/sec)
W	weight, N (lb)
x	chordwise station measured from basic airfoil nose, percent chord
X	body reference axis, wing root-chord line
Y	body reference axis, normal to reflection plane
z	distance normal to wing-chord plane, percent chord
Z	body reference axis, normal to wing-chord plane
α	angle of attack, deg
γ	flight-path angle, $-\tan^{-1}(C_D/C_L)$, deg
δ_f	flap deflections measured streamwise, deg
δ_j	jet turning angle, deg

APPARATUS AND MODEL

The tests were conducted in a 3.7-m (12-ft) tunnel using the setup illustrated in figure 2. The reflection plane was 2.44 m (8 ft) long and 2.13 m (7 ft) wide and the model was mounted in the center.

The investigation was conducted using the basic semispan model of reference 3, but with the two pod-mounted engines moved to the upper surface of the wing as shown in figure 3. The wing had a plain trailing-edge flap with an extension added which nearly doubled the original flap chord, and a $0.25c_w$ leading-edge Krueger flap extending from the outboard side of the engine nacelle to the wing tip. The added area of the flap extension was not included in the reference values of S, $\bar{c}$, and A. It is envisioned that this extension would be mechanically linked to the flap and would extend when the flap was lowered. The dimensional characteristics of the model are presented in table I and in the sketches of figures 3 and 4. Details of the wing section and BLC system are shown in figure 4(a) and the airfoil section coordinates are given in table II. The trailing-edge flap was fabricated in three equal length spanwise segments which could be deflected individually. High pressure BLC air was ducted spanwise by a tapered tube mounted in the wing just ahead of the flap and was blown rearward through 96 small holes drilled in the tube. The holes had a diameter of 0.2 percent of the local wing chord and a spanwise spacing of 4 percent of the local chord. The blowing air impinged on the upper surface of the flap near its leading edge and passed through a small gap between the flap and a flat metal sheet mounted on the wing trailing edge. For the midspan and outboard flap elements, the flat metal sheet was flexibly mounted so that the gap size was determined by the blowing pressure used (the gap was closed when no blowing was used). For the inboard flap element (behind the engines) the flat metal sheet was rigidly mounted on the wing so that a gap size of 0.0762 cm (0.03 in.) was maintained regardless of the blowing pressure. For a majority of the tests, blowing was used on the midspan and outboard flaps only and for these tests the inboard BLC was closed.

The turbofan engines were simulated on the model by tip-jet driven ducted fans. (See fig. 4(b).) Their size, relative to that of the wing, represented approximately the size of high-bypass-ratio turbofan engines capable of providing a thrust-weight ratio of 0.60 for a representative STOL jet transport. Two identical nacelles such as that sketched in figure 4(b) were mounted together in a siamese pod on the upper surface of the wing. Several different exhaust deflectors (see fig. 4(c)) were attached to the top of the nacelles to spread the jet efflux into a thin sheet. Tests were made to determine the effect of these deflectors on the turning of the jet over the flap. Deflector lengths of 7.62 cm (3 in.), 12.70 cm (5 in.), and 22.86 cm (9 in.) were investigated and each deflector was set to provide an exhaust exit gap of 2.54 cm (1 in.) and 5.08 cm (2 in.). Following preliminary tests with all of the deflectors, the main body of the test program was then run with a 12.70-cm (5-in.) deflector with a gap of 5.08 cm (2 in.). It should be noted that the deflectors were open on each side to minimize reductions in the engine exit area and to promote spanwise spreading of the jet.

TESTS

Preliminary tests at zero angle of attack were conducted to determine the individual effects of exhaust-deflector length, exhaust-deflector gap, and blowing boundary-layer control on each of two general trailing-edge flap configurations: (1) a take-off configuration with the full-span flap deflected 30° and (2) a landing configuration with the inboard, midspan, and outboard flap segments deflected 60°, 50°, and 30°, respectively. The main body of the test program was then conducted for these two flap configurations over an angle-of-attack range for several different thrust coefficients using a deflector and BLC combination selected from the preliminary studies.

In preparation for the tests, the engines were calibrated to determine gross thrust as a function of engine rotational speed in the static condition with the exhaust deflector off. The tests were then run by setting the engine rotational speed to give the desired thrust and holding speed constant through the angle-of-attack range. A check was made to determine whether forward speed had any significant effect on the gross thrust. These tests were made by determining the effect of forward speed on the total pressure in the nozzle for a given rotational speed. The total pressure was measured by eight total pressure tubes immediately behind the fan.

The boundary-layer blowing momentum was measured under static conditions with the trailing-edge flap in place, but with a ramp on the knee of the flap to keep the airflow from attaching to the flap during the calibration.

Tests were run at approximately the following conditions:

$V = 10.7$ m/sec (35 ft/sec)

$q = 68$ N/m^2 (1.42 lb/ft^2)

$R = 0.31 \times 10^6$

CORRECTIONS

Wind-tunnel wall corrections (determined from a previous investigation with a high-lift model in the tunnel) were applied to the data. These corrections were determined experimentally by placing the model and test assembly of reference 3 in the 9- by 18-m (30- by 60-ft) test section of the Langley full-scale tunnel. The following equations were obtained from reference 3 and the corrections applied to the data:

$$\alpha = \alpha' + 0.579C_L'$$

$$C_D = C_D' + 0.0101C_L'^2$$

$$C_L = C_L' - 0.0101C_L'C_D'$$

where primes indicate uncorrected values. Total pressure measurements of the engines indicated that for the speeds used in the test there was no measurable effect of forward speed on the total pressure and, presumably, on the gross thrust.

RESULTS AND DISCUSSION

Preliminary Tests

Wind off.- The results of wind-off tests to determine the jet turning angle and turning efficiency $\left(\sqrt{\frac{F_A^2 + F_N^2}{T^2}}\right)$ for the model in several different configurations are presented in figures 5 and 6 in terms of the ratio of normal force to thrust F_N/T plotted against the ratio of net axial force to thrust F_A/T. The data of figure 5(a) show that the turning efficiency and turning angle for the landing flap configuration $(\delta_f = 60^o, 50^o, 30^o)$ varied considerably with deflector length and deflector gap. For the conditions tested the highest turning angle measured was only about 55^o, indicating that the jet was not following the upper contour of the flap very well. It should be noted, however, that tufts attached to the flap upper surface showed that the surface flow was attached to the flap.

These efficiencies are based upon the gross thrust of the engine and do not, therefore, account for thrust losses resulting from the installation of an exhaust deflector. On the basis of the engine total pressure measurements, it was observed that the longer deflectors with the 5.08-cm (2-in.) exhaust gap showed only a small effect on the gross thrust of the engine. The high (80 to 85 percent) turning efficiencies indicated in figure 5(a) for these arrangements are therefore indicative of the efficiencies that may be expected for the USB. Reducing the exhaust gap to 2.54 cm (1 in.) or shortening the deflector length to 7.26 cm (3 in.) showed large changes in the total pressure inside the engines, indicating that these arrangements were back-pressuring the engines and thereby causing losses in the basic engine thrust.

The low efficiencies shown in figure 5(a) for these arrangements are, therefore, most likely a result of the thrust loss and are not a true indication of the effectiveness of these deflectors for spreading and turning the jet efflux. The data of figure 5(b) show that jet turning angles of only about 20^o to 25^o were possible with the deflectors removed and without boundary-layer control; but the use of boundary-layer control at the knee of the flap helped to increase the turning angle for this condition. Figure 6 shows that the take-off flap configuration $(\delta_f = 30^o, 30^o, 30^o)$ was much more effective for turning the jet than the landing flap configuration $(\delta_f = 60^o, 50^o, 30^o)$. For example, the turning angle for the take-off configuration was approximately 45^o, which is approximately the deflection angle

of the upper surface of the flap, indicating that the jet efflux for this case was following the flap very closely.

Wind on.- In order to determine the effectiveness of the exhaust deflectors in the wind-on conditions, the deflectors were tested at $\alpha = 0^{o}$ for several values of C_{μ} and the results are presented in figures 7 and 8 for gap heights of 5.08 and 2.54 cm (2 and 1 in.), respectively. The results of these figures show that the deflectors, as expected, increased the lift performance of the model and, when boundary-layer control was added, all of the deflectors produced about the same lift performance for a given gap height and thrust coefficient. The primary effect of deflector gap was that the 2.54-cm (1-in.) gap resulted in higher drag of the model, probably because of the poorer turning efficiency for this gap height (see fig. 5(a)). Because of this effect, the 5.08-cm (2-in.) gap was chosen along with the 12.70-cm (5-in.) deflector for use in the test program. It should be noted that, although exhaust-gap heights of 2.54 cm (1 in.) showed marked reductions in turning efficiency when compared to the 5.08-cm (2-in.) heights, approximately the same amount of lift was obtained with all of the deflectors tested. While the precise mechanics of this characteristic are not known at the present time the relative insensitivity of lift to the lower turning efficiencies of the 2.54-cm (1-in.) height is apparently due to the increased spanwise spreading of the exhaust through the open sides of the deflector. This spreading results in the fact that a larger portion of the span is affected by the exhaust jet, thereby increasing the area and effective aspect ratio of the jet-augmented region of the wing.

Lift Characteristics

It should be pointed out that in the present study the majority of the basic tests was made with boundary-layer control on the outer span of the wing only. For the values of engine C_{μ} used in these tests $\left(C_{\mu} = 2.095 \text{ and } 4.24\right)$, there was no problem with turning of the jet exhaust sheet for either the take-off or landing flap settings, provided the wing-flap juncture behind the engines was faired smoothly to close the BLC gap and to eliminate surface roughness. It was found during the latter part of the test program, however, that even with the flap faired smoothly, the jet exhaust sheet separated from the flap at low values of C_{μ}, causing large abrupt losses in lift. This result is very similar to that pointed out in earlier work with the USB (ref. 2) and is a function of the jet velocity, jet height, and flap turning radius. In all cases, the use of blowing boundary-layer control at the flap knee eliminated this problem and produced satisfactory turning conditions for the range of thrust coefficients and flap angles investigated. This point is illustrated in a plot of lift coefficient against thrust coefficient in figure 9. This figure shows that for the condition of $C_{\mu,BLC} = 0$, the jet exhaust sheet separated from the flap below a value of C_{μ} of approximately 1.3 for a deflector gap of 5.08 cm (2 in.). Reducing the deflector gap to 2.54 cm (1 in.) reduced the value of C_{μ} at which flow separation occurred to

about 0.5. The shaded area at the lower end of the curves for $C_{\mu,BLC} = 0$ indicates a region in which there was a hysteresis effect depending on whether C_μ was being increased or decreased. It should be pointed out that these data were obtained with the wing-flap juncture faired smoothly. In tests in which the fairing was removed from the flaps behind the engines, it was found that the critical value of C_μ for flow attachment was much higher and that the hysteresis effect was much more pronounced than those shown in figure 9. For both of the gap heights tested, a small amount of BLC blowing at the flap knee resulted in flow attachment in the critical C_μ range shown in figure 9. For values of C_μ above the critical range, blowing on the flap directly behind the engine produced only small increases in the performance of the model. This point was determined by comparing preliminary results of tests having full-span blowing with those having blowing on the outer span of the wing only.

The basic longitudinal data for the landing and take-off flap configurations are presented in figures 10 to 13 and summarized in the form of lift-drag polars in figures 14 and 15. The basic data plots show that the stall angle of attack and the maximum lift coefficient increased with increasing thrust coefficient. The data of figures 10 and 11 show that lift coefficients up to about 10 (untrimmed) could be produced for a gross thrust coefficient of 4.24. The use of boundary-layer control at the knee of the trailing-edge flap increased the maximum lift coefficient up to about 10.7 for $C_{\mu,BLC} = 0.140$ (see fig. 11). As would be expected, the high lift coefficients were accompanied by diving moments. An examination of figures 14 and 15 shows that the use of boundary-layer control produced better performance in terms of the available lift coefficient for a given glide or climb angle.

Figure 16 is a comparison of the trim lift and drag characteristics of the USB model of the present investigation with those for an externally blown jet-flap model from reference 4. These results show that the present model was more efficient for producing lift for a given amount of thrust than was the externally blown jet-flap model.

Longitudinal Stability and Trim

The tail-off longitudinal stability can be determined from the basic pitching-moment plots in figures 10 to 13. These data show, as expected, an increase in diving moments and an increase in positive slope of the pitching-moment curves (indicating an increase in longitudinal instability) with increasing thrust coefficient. For convenience in comparison, a plot of the pitching-moment data of the present investigation together with data for the externally blown flap (EBF) from reference 4 is presented in figure 17. A comparison of these data indicates that, for a given thrust coefficient and center-of-gravity location, the two concepts showed about the same diving moments at zero angle of attack but that the USB model had slightly more instability than the EBF model. In comparing the data of figure 17, it should be remembered that for a given thrust coefficient, the

USB model produced more lift than did the EBF model (see fig. 16). This result means that even though the two concepts showed about the same diving moments for a given thrust coefficient, the flap center of pressure for the USB model was more forward on the wing. This point is illustrated in figure 18, which shows the variation of the locations of the wing-flap center of pressure and wing-body aerodynamic center as a function of thrust coefficient. From this plot it is seen that the center of pressure and aerodynamic center for the USB model were about 10 percent more forward on the wing than those for the EBF model. This difference in center of pressure and aerodynamic center for the two models can be attributed mainly to the fact that the externally blown flap had a double-slotted flap which extended much more rearward than did the plain flap on the present model.

Performance

A flight envelope (curve of flight-path angle as a function of lift coefficient for various thrust-weight ratios) prepared from the data of figure 10(b) is shown in figure 19. The BLC blowing momentum for these data was sufficient to attach the flow, $C_{\mu,BLC} = 0.061$. This momentum coefficient is easily obtainable with the advanced technology, high-bypass-ratio (15 to 20) turbofans anticipated for use on STOL aircraft having nominal thrust-weight ratios of 0.6 and fan pressure ratios near 1.15. The critical maneuver for this type aircraft is a wave-off and go-around with full power, at approach speed, and with one engine inoperative. For a four-engine STOL transport with an installed thrust-weight ratio of 0.6, this corresponds to operation at a thrust-weight ratio of 0.45. Figure 19 shows a maximum lift coefficient of about 9.9 at this thrust-weight ratio for $C_{\mu,BLC} = 0.061$ and $\delta_f = 60^o, 50^o, 30^o$.

After allowing a 30-percent speed margin above the stall speed, the maximum lift coefficient for full-power, three-engine operation is about 5.8. Figure 19 indicates that virtually no climb capability exists under these conditions, particularly when the drag associated with roll trim is considered.

A comparison of figures 14 and 15 indicates that by raising the flaps from the landing position $(\delta_f = 60^o, 50^o, 30^o)$ to the take-off position $(\delta_f = 30^o, 30^o, 30^o)$, some climb capability is obtained for a wave-off condition, although some angle-of-attack adjustment is required through the transition.

Figure 20 presents data from references 5 and 6 and the present study and indicates the thrust-weight ratio required for straight and level flight at a given lift coefficient. In figure 20 the thrust-weight ratio $C_\mu/C_{L,trim}$ is a measure of engine size, for which $C_\mu/C_{L,trim}$ is the closest equivalent in jet-flap studies. The trends shown indicate that while the USB model requires considerably more thrust than the augmentor-wing model of reference 6, it requires a smaller amount of thrust than the external-flow model of

reference 5. Such a direct comparison with the augmentor-wing concept is perhaps not valid since the augmentor-wing concept presumably will require a lower-bypass-ratio engine. This has considerable impact on engine weight, fuel consumption, and noise and should be considered in any comparison of these systems.

SUMMARY OF RESULTS

From a wind-tunnel investigation of a semispan model of a STOL jet transport with an upper-surface blown jet flap and blowing boundary-layer control, the following results were obtained:

1. The results of the investigation showed that the high lift coefficients necessary for STOL operation could be achieved with the test configuration and that the performance was comparable to that of other powered-lift STOL concepts.

2. The combination of engine exhaust deflectors and blowing boundary-layer control was found to be effective for maintaining flow attachment over the flaps for the entire operational envelope.

3. The use of a plain flap behind the engine, which appears from previous work to have an advantage in reducing the perceived noise level, resulted in lower diving moments than those associated with more complicated flap systems.

Langley Research Center,
National Aeronautics and Space Administration,
Hampton, Va., April 19, 1973.

REFERENCES

1. Voedisch, Alfred, Jr.: Analytical Investigation of the Coanda Effect. Tech. Rep. F-TR-2155-ND (ATI No. 9881), Air Materiel Command, U.S. Air Force, Apr. 3, 1947.

2. Turner, Thomas R.; Davenport, Edwin E.; and Riebe, John M.: Low-Speed Investigation of Blowing From Nacelles Mounted Inboard and on the Upper Surface of an Aspect-Ratio-7.0 35° Swept Wing With Fuselage and Various Tail Arrangements. NASA MEMO 5-1-59L, 1959.

3. Henderson, Robert L.: Low-Speed Wind-Tunnel Investigation of a Semispan STOL Jet Transport Wing With Deflected Thrust and Blowing Boundary-Layer Control. NASA TN D-6256, 1971.

4. Freeman, Delma C., Jr.; Parlett, Lysle P.; and Henderson, Robert L.: Wind-Tunnel Investigation of a Jet Transport Airplane Configuration With an External-Flow Jet Flap and Inboard Pod-Mounted Engines. NASA TN D-7004, 1970.

5. Parlett, Lysle P.; Greer, H. Douglas; Henderson, Robert L.; and Carter, C. Robert: Wind-Tunnel Investigation of an External-Flow Jet-Flap Transport Configuration Having Full-Span Triple-Slotted Flaps. NASA TN D-6391, 1971.

6. Falarski, Michael D.; and Koenig, David G.: Aerodynamic Characteristics of a Large-Scale Model With a Swept Wing and Augmented Jet Flap. NASA TM X-62,029, 1971.

TABLE I.- DIMENSIONS OF MODEL

Wing:	
Area, m^2 (ft^2)	0.521 (5.61)
Semispan, cm (in.)	142.88 (56.25)
Semispan aspect ratio	3.92
Length of mean aerodynamic chord, cm (in.)	39.12 (15.40)
Location of quarter chord of mean aerodynamic chord, referenced to root-chord leading edge, cm (in.)	34.70 (13.66)
Spanwise location of mean aerodynamic chord, cm (in.)	59.44 (23.40)
Root chord, cm (in.)	50.80 (20.00)
Tip chord, cm (in.)	19.05 (7.50)
Break-station chord, cm (in.)	50.80 (20.00)
Spanwise station of break station, cm (in.)	14.22 (5.60)
Sweep of quarter-chord line:	
Inboard panel, deg	0
Outboard panel, deg	25.00
Dihedral, deg	0
Geometric twist, deg	0
Basic airfoil	NACA 65_1-412
Trailing-edge flap:	
Root chord, cm (in.)	15.24 (6.00)
Tip chord, cm (in.)	5.72 (2.25)
Hinge-line station, percent chord	77
Sweep of hinge line, deg	17.5
Flap leading-edge radius at root, cm (in.)	2.59 (1.02)
Flap leading-edge radius at tip, cm (in.)	0.965 (0.38)
Length of flap extension at root, cm (in.)	13.97 (5.50)
Length of flap extension at tip, cm (in.)	5.23 (2.06)
Flap extension angle, referenced to chord line, deg	16.7
BLC:	
Gap station on upper surface, percent chord	77
Blowing tube inside diameter, percent chord	2.0 to 2.5
Blowing hole spacing along tube, percent chord	4.0
Blowing hole diameter, percent chord	0.20
Blowing-jet inclination to chord line, deg	0 (approx)
Blowing-jet inclination to reflection plane, deg	0 (approx)
Krueger flap:	
Root chord, percent local wing chord	25
Tip chord, percent local wing chord	25
Deflection from wing, deg	110
Engines:	
Inlet diameter, cm (in.)	15.24 (6.00)
Exit width, cm (in.)	19.30 (7.60)
Exit area, cm^2 (in^2)	331.00 (51.30)
Length, inlet face to exit center, cm (in.)	32.00 (12.60)
Inboard engine center line to wing root, cm (in.)	25.91 (10.20)
Outboard engine center line to wing root, cm (in.)	50.29 (19.80)
Engine center line above wing chord	6.4 (2.5)
Engine inlet ahead of $0.50\bar{c}$	52.0 (20.5)

TABLE II.- AIRFOIL COORDINATES FOR WING AND FLAP

Wing (with Krueger flap and slat removed)			Flap (no deflection)		
x, percent chord	z_{upper}, percent chord	z_{lower}, percent chord	x, percent chord	z_{upper}, percent chord	z_{lower}, percent chord
3.50	-0.55	-0.55	72.00	0	0
4.00	.50	-1.80	72.50	1.50	-1.45
5.00	1.55	-2.00	73.00	2.40	-1.40
7.50	3.25	-2.40	74.00	3.40	-1.30
10.00	4.30	-2.60	77.00	4.50	-1.00
12.50	5.35	-2.95	82.00	4.60	-.50
15.00	5.75	-3.03	87.00	3.85	-.05
20.00	6.57	-3.35	92.00	2.50	.15
30.00	7.66	-3.76	100.00	0	0
40.00	8.14	-3.86	Flap extension		
50.00	7.96	-3.55			
60.00	7.09	-2.79	100.00	0	
70.00	5.70	-1.78	126.34	-7.90	
80.00	3.95	-.74	Hinge line		
90.00	1.98	.09			
100.00	0	0	76.85	-0.20	

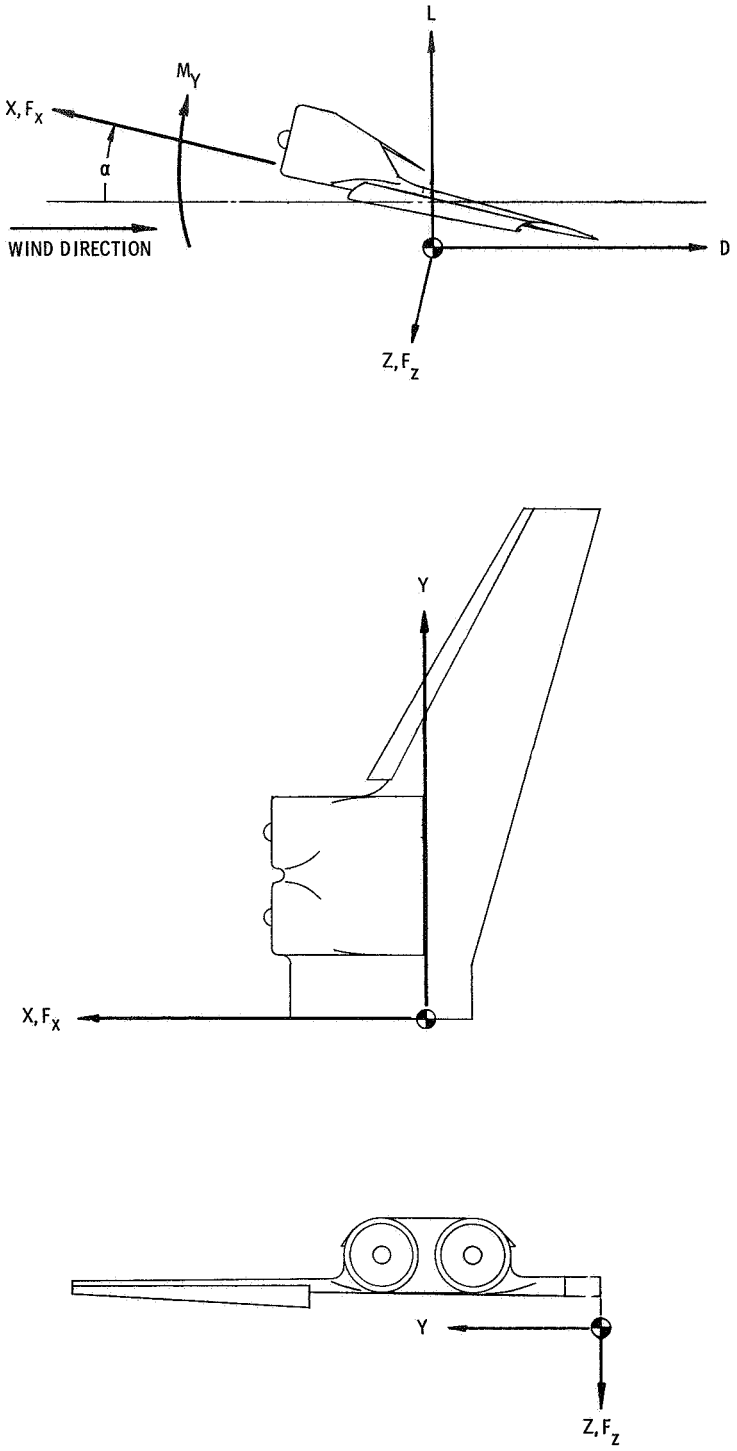

Figure 1.- Axis system used in presentation of data. Arrows indicate positive direction of forces and moments.

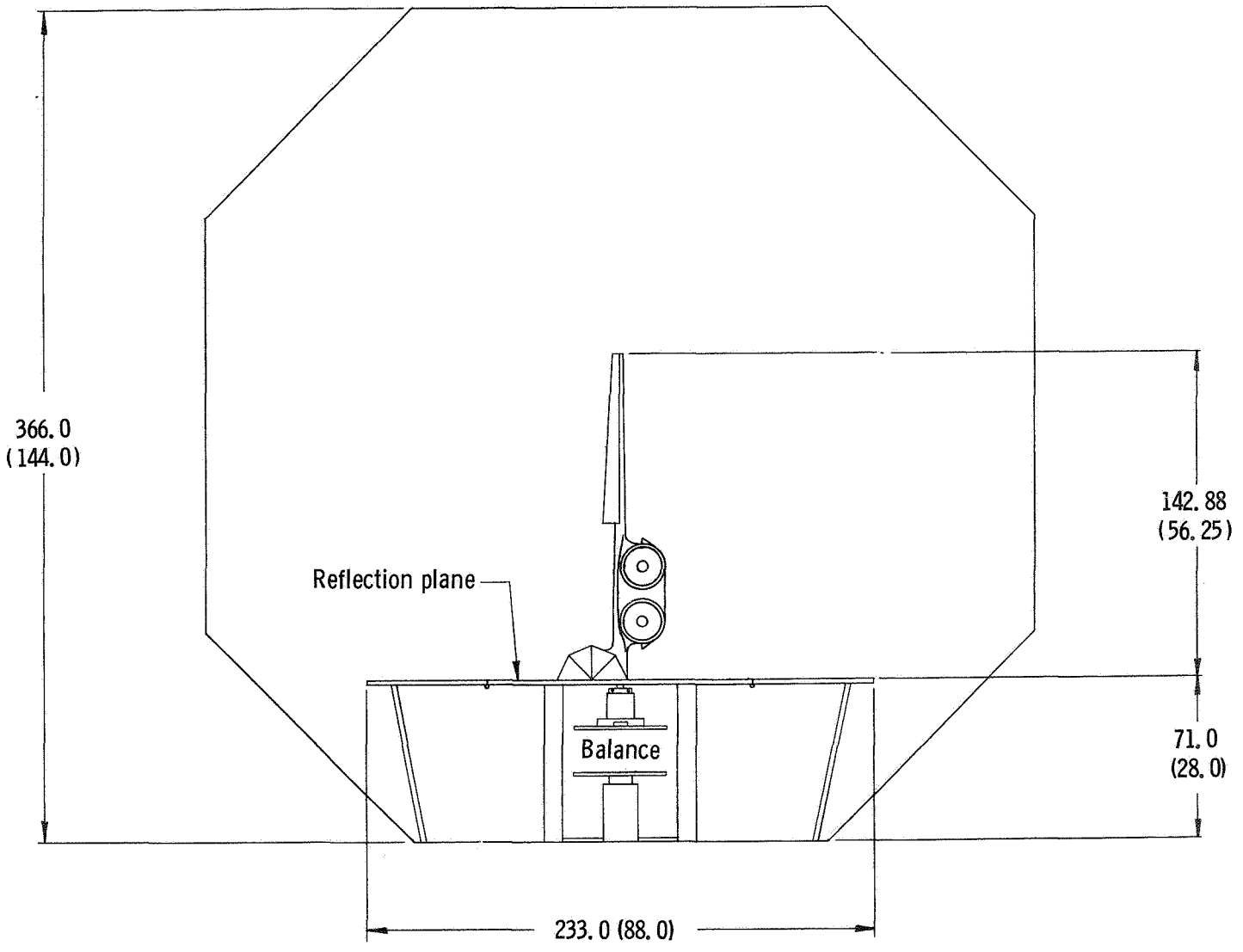

Figure 2.- Setup in 3.7-m (12-ft) low-speed wind tunnel. Dimensions are given in centimeters (in.).

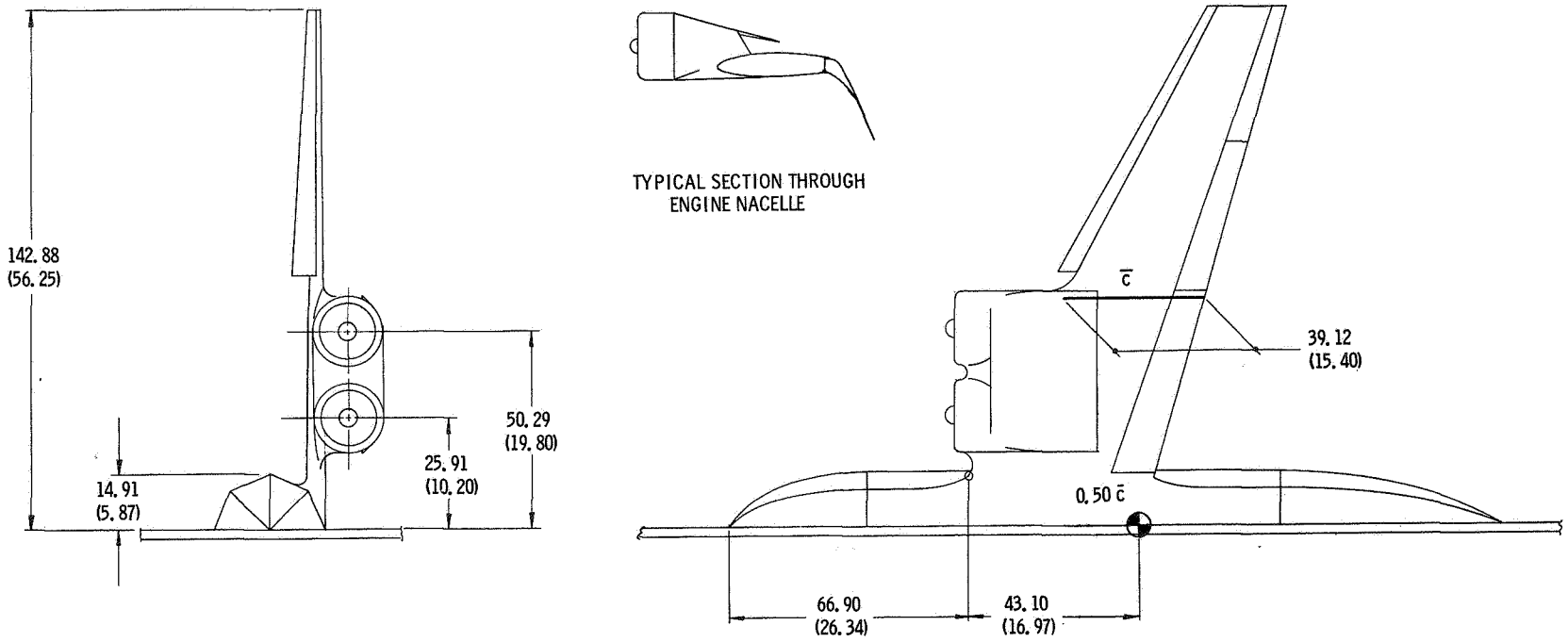

Figure 3.- Model used in test. Dimensions are given in centimeters (in.).

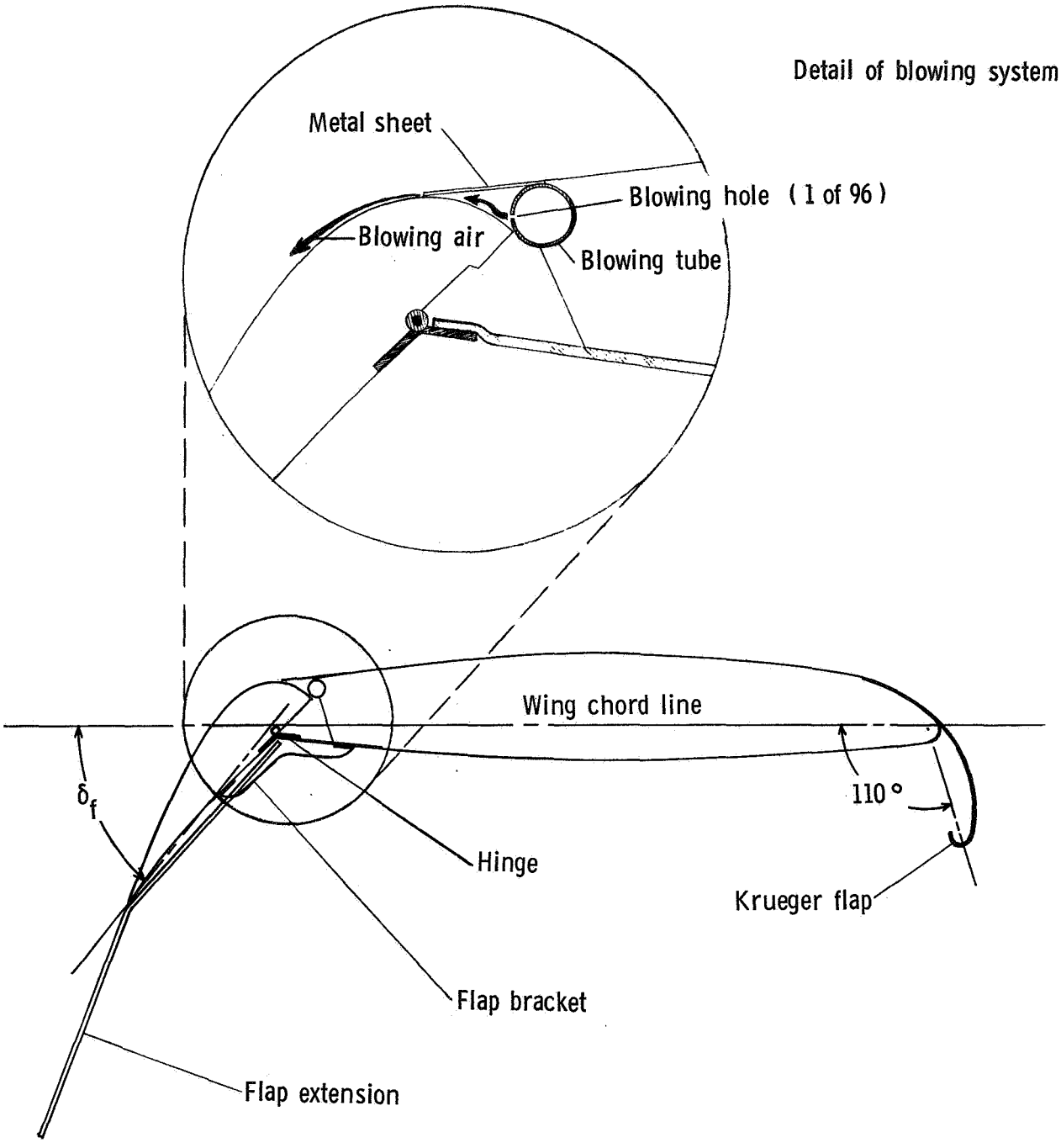

(a) Wing section.

Figure 4.- Wing and engine details. Dimensions are given in centimeters (in.).

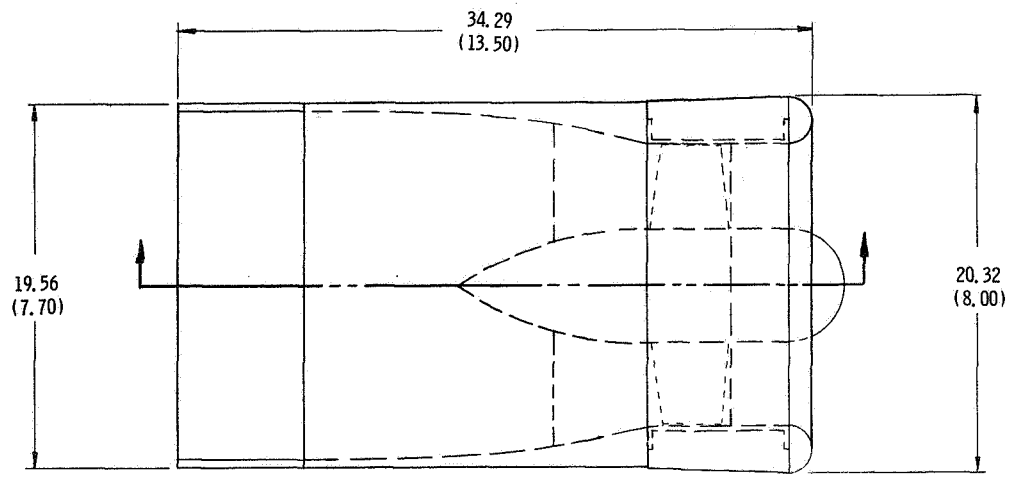

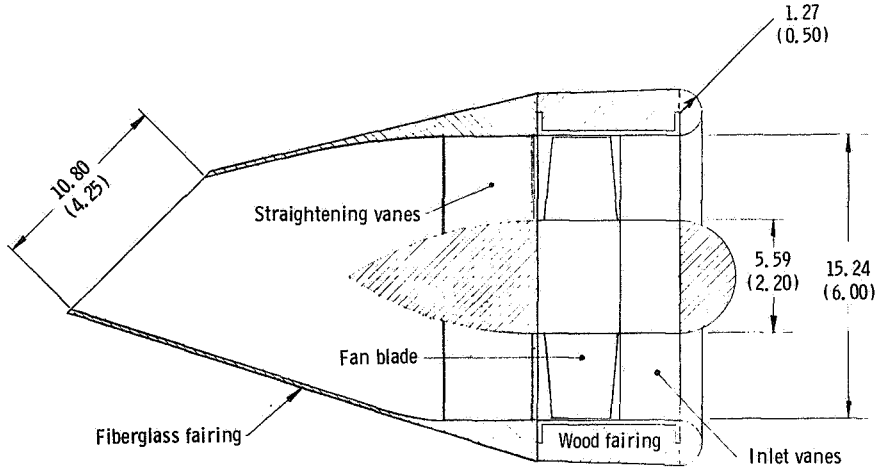

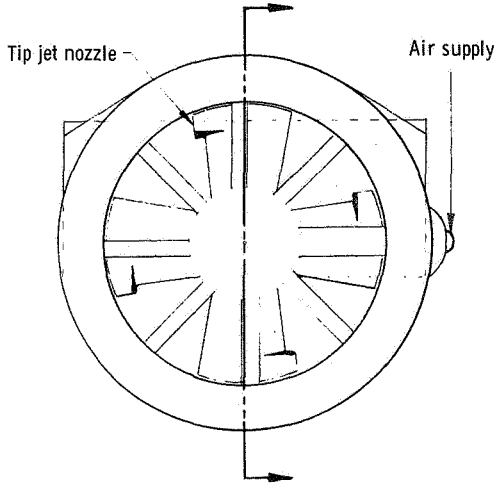

(b) Engine nacelles.

Figure 4.- Continued.

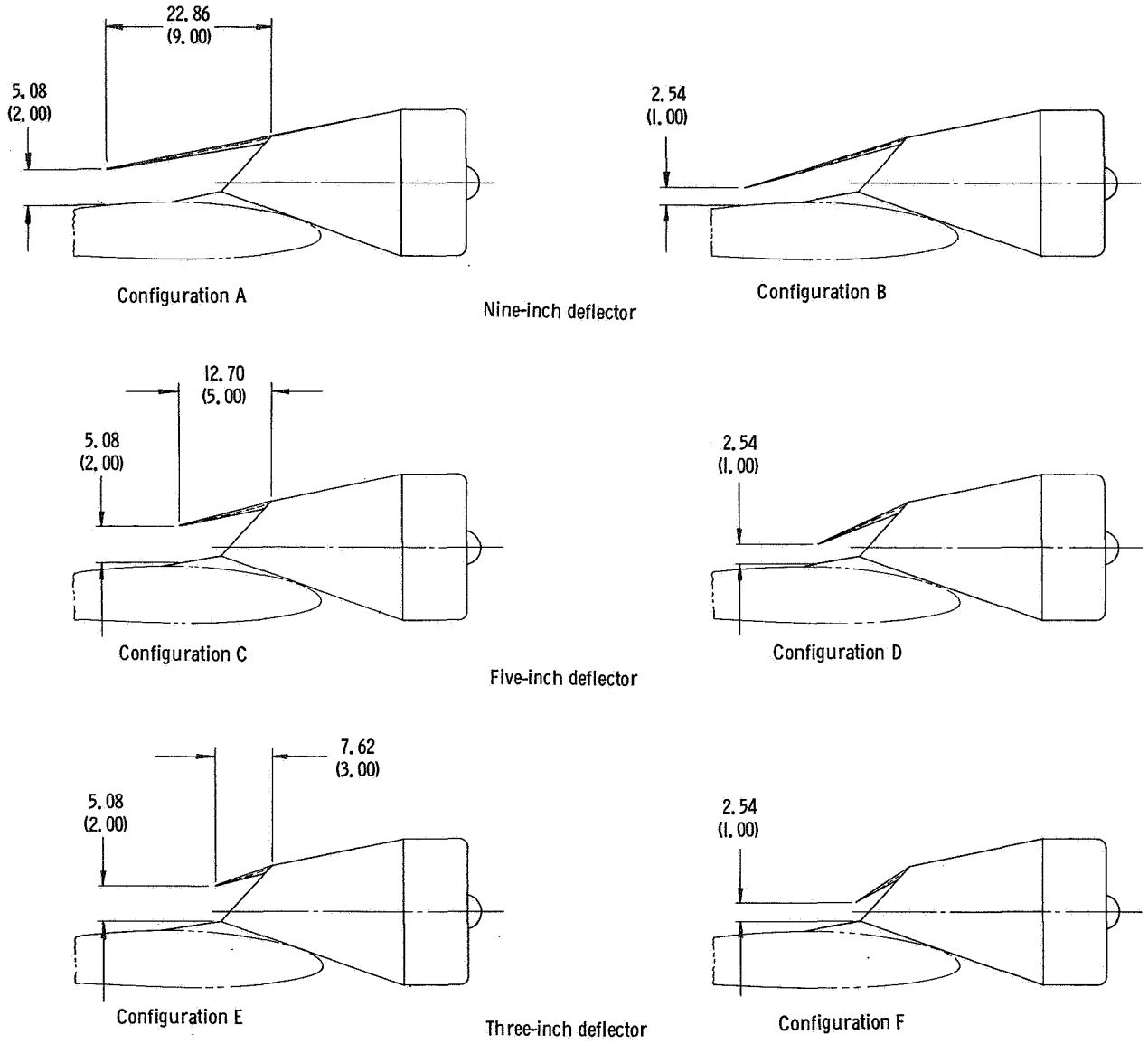

(c) Deflectors.

Figure 4.- Concluded.

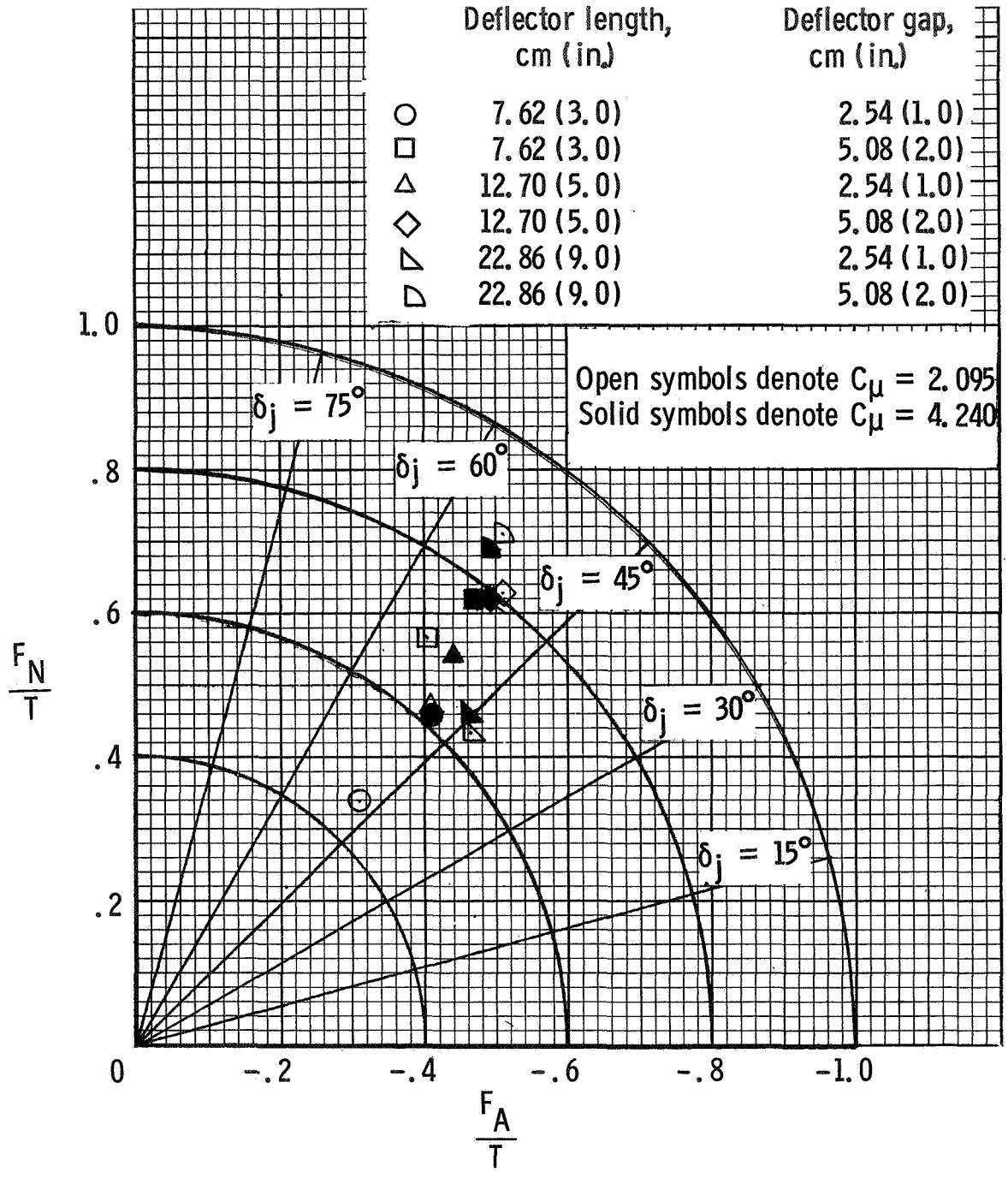

(a) $C_{\mu,BLC} = 0.$

Figure 5.- Summary of flap turning efficiency and turning angle. Landing flap configuration $(\delta_f = 60^o, 50^o, 30^o)$.

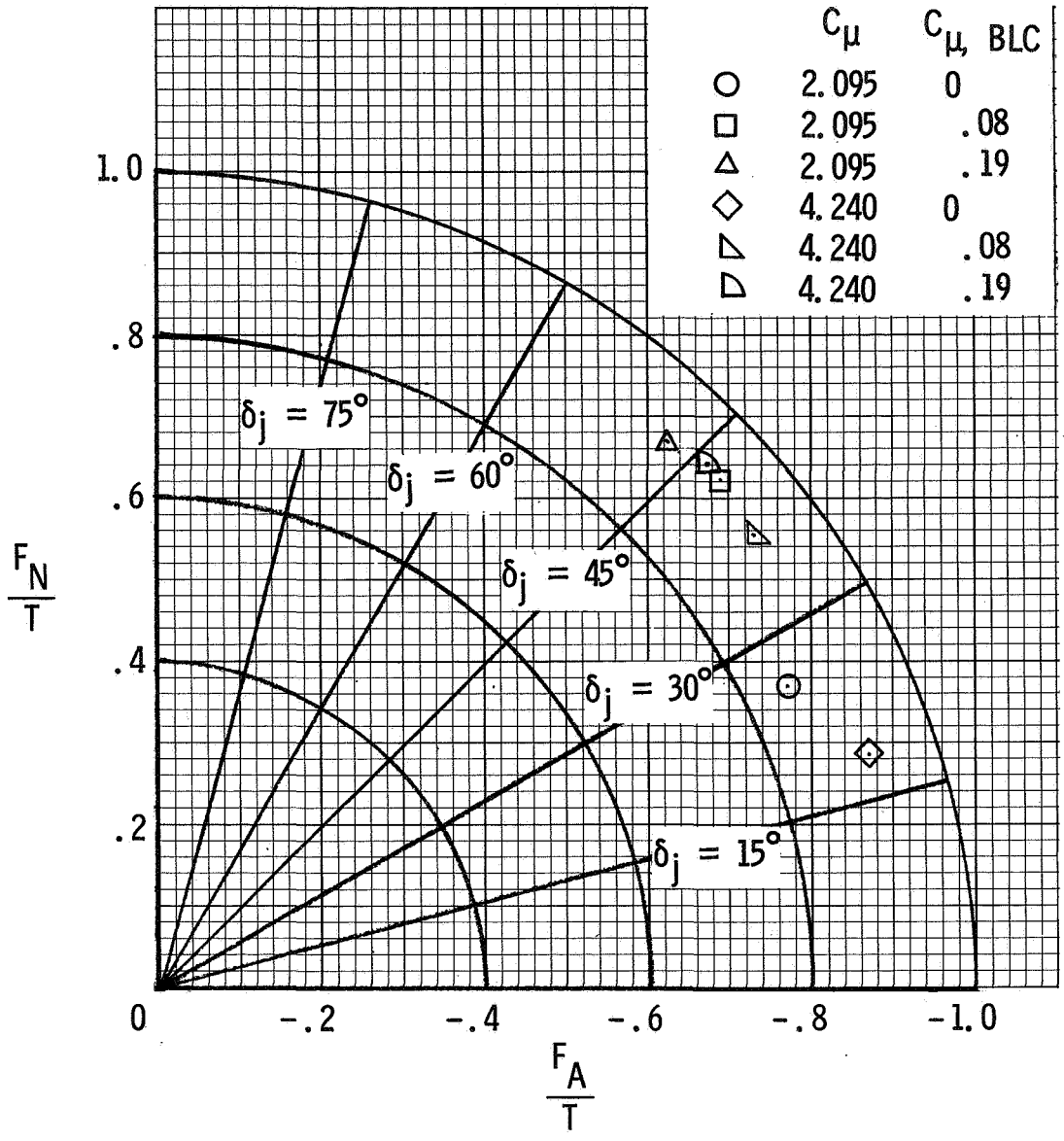

(b) Deflectors off.

Figure 5.- Concluded.

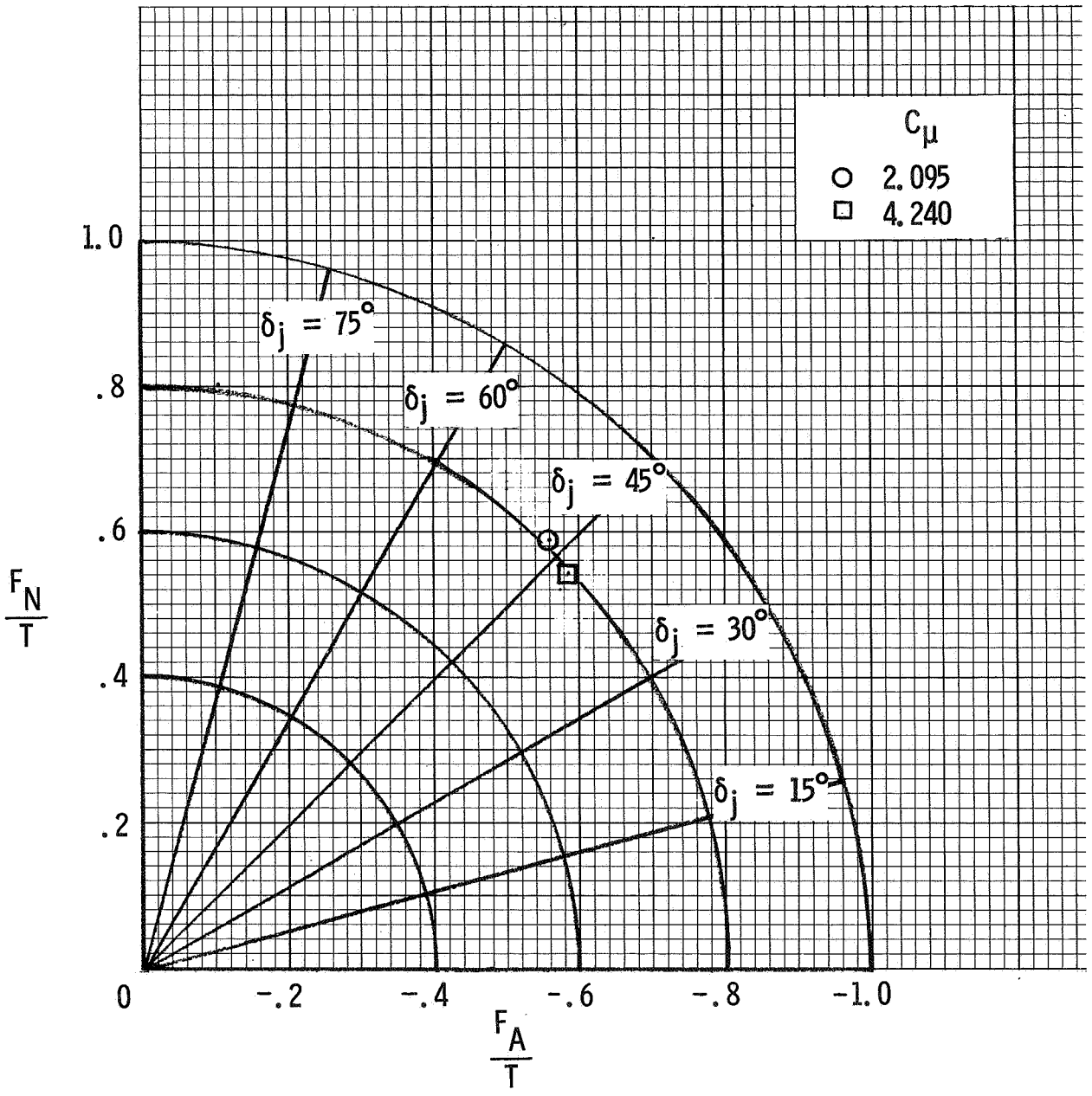

Figure 6.- Summary of flap turning efficiency and turning angle. Take-off flap configuration ($\delta_f = 30^o, 30^o, 30^o$); $C_{\mu,BLC} = 0$; deflector length = 12.70 cm (5.0 in.); deflector gap = 5.08 cm (2.0 in.).

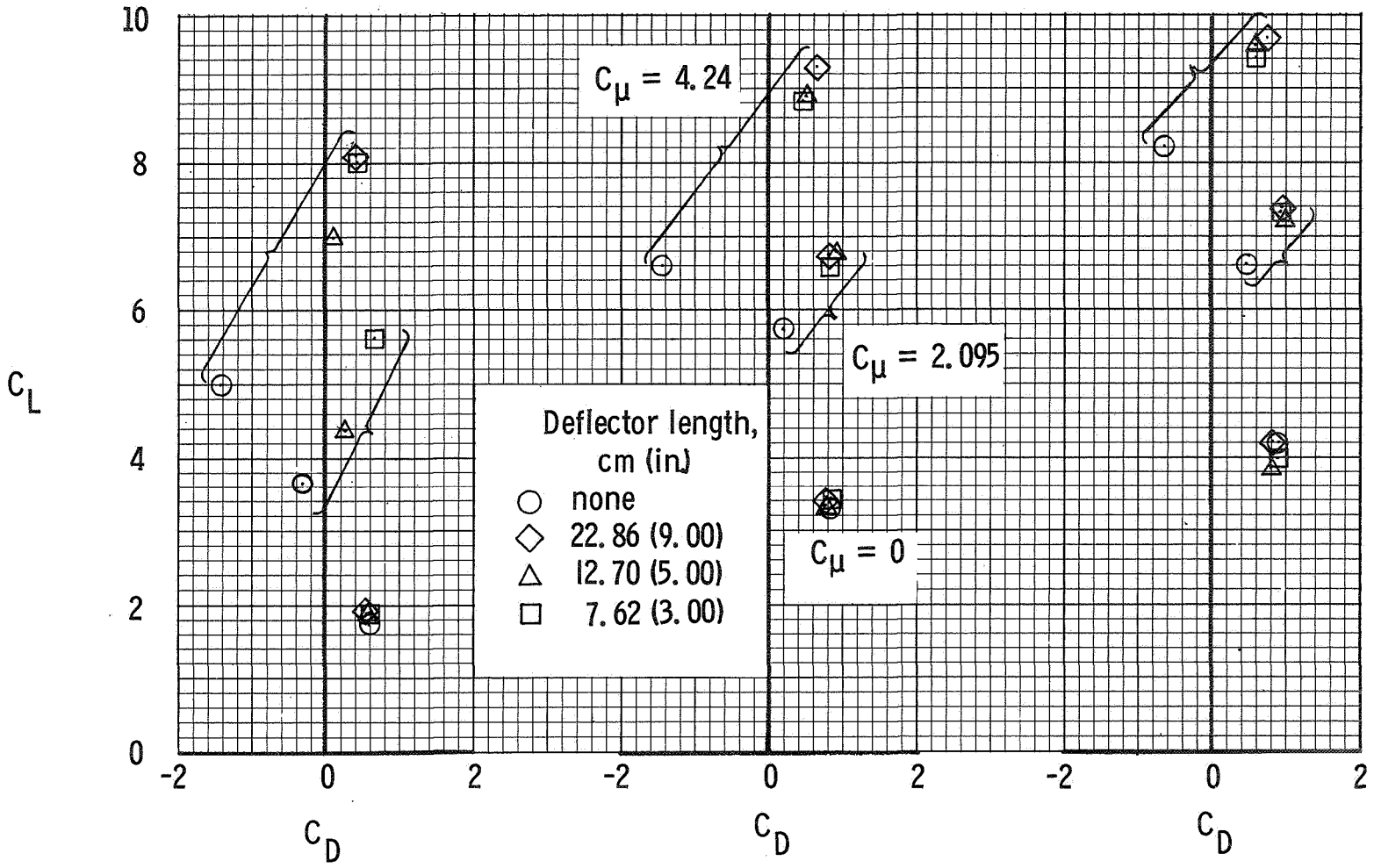

(a) $C_{\mu,BLC} = 0$. (b) $C_{\mu,BLC} = 0.08$. (c) $C_{\mu,BLC} = 0.19$.

Figure 7.- Effect of engine exhaust deflector on the lift and drag characteristics of the model. Landing flap configuration ($\delta_f = 60^o, 50^o, 30^o$); deflector gap = 5.08 cm (2 in.).

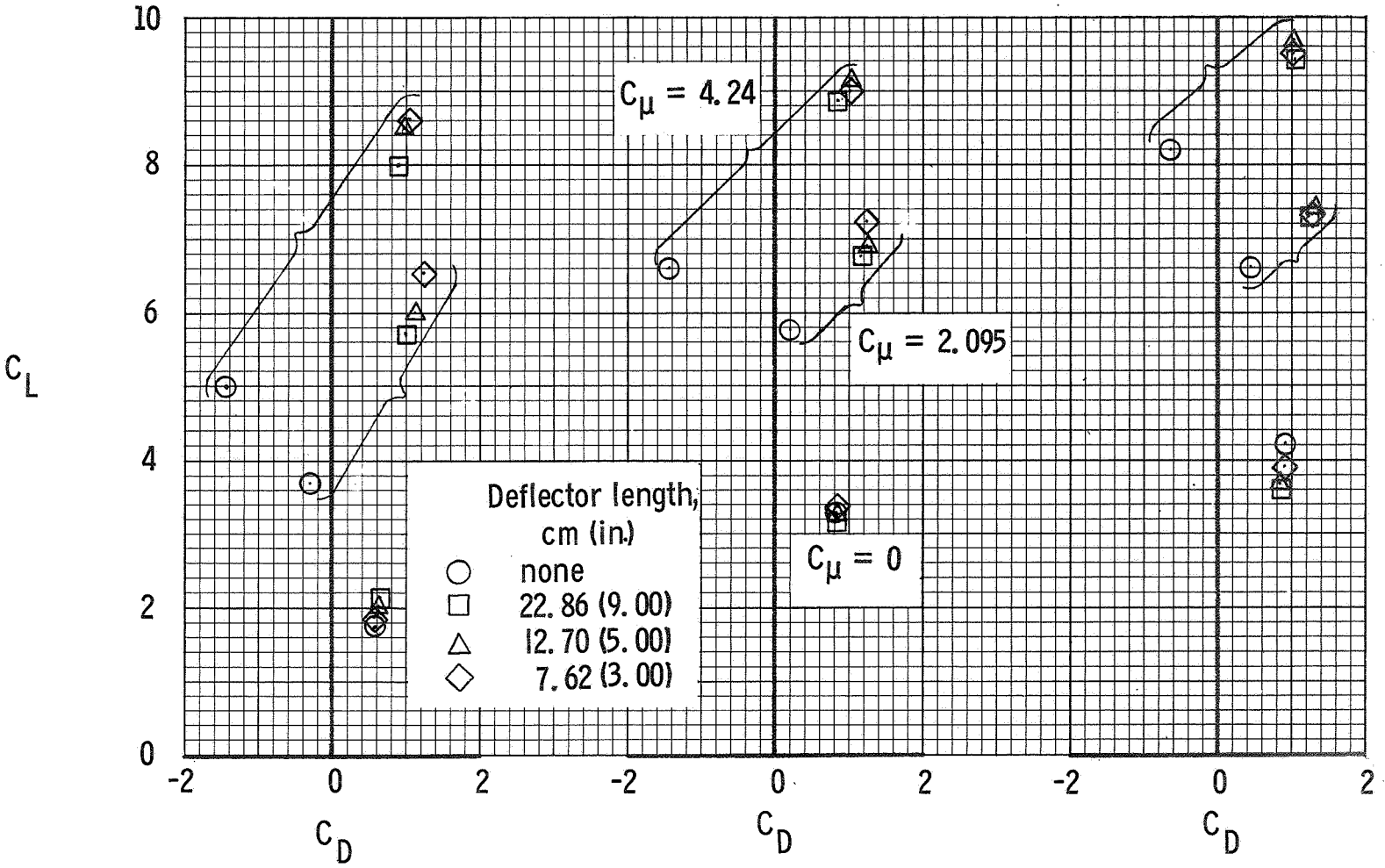

(a) $C_{\mu,BLC} = 0.$ (b) $C_{\mu,BLC} = 0.08.$ (c) $C_{\mu,BLC} = 0.19.$

Figure 8.- Effect of engine exhaust deflector on the lift and drag characteristics of the model. Landing flap configuration ($\delta_f = 60^o, 50^o, 30^o$); deflector gap = 2.54 cm (1 in.).

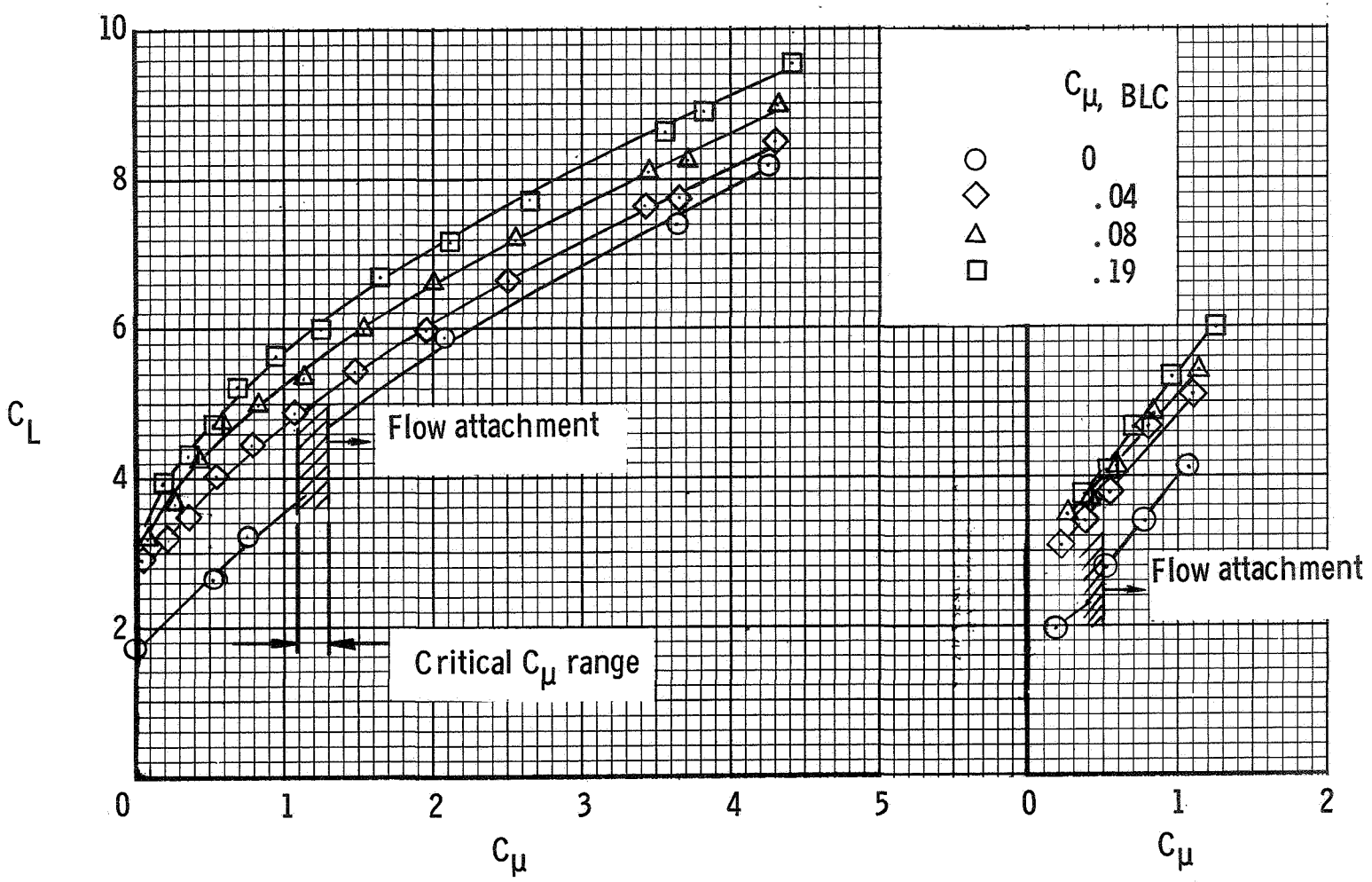

(a) Deflector gap = 5.08 cm (2 in.).

(b) Deflector gap = 2.54 cm (1 in.).

Figure 9.- Effect of blowing boundary-layer control on the lift characteristics of the model. Deflector length = 12.70 cm (5.0 in.); landing flap configuration ($\delta_f = 60^o, 50^o, 30^o$).

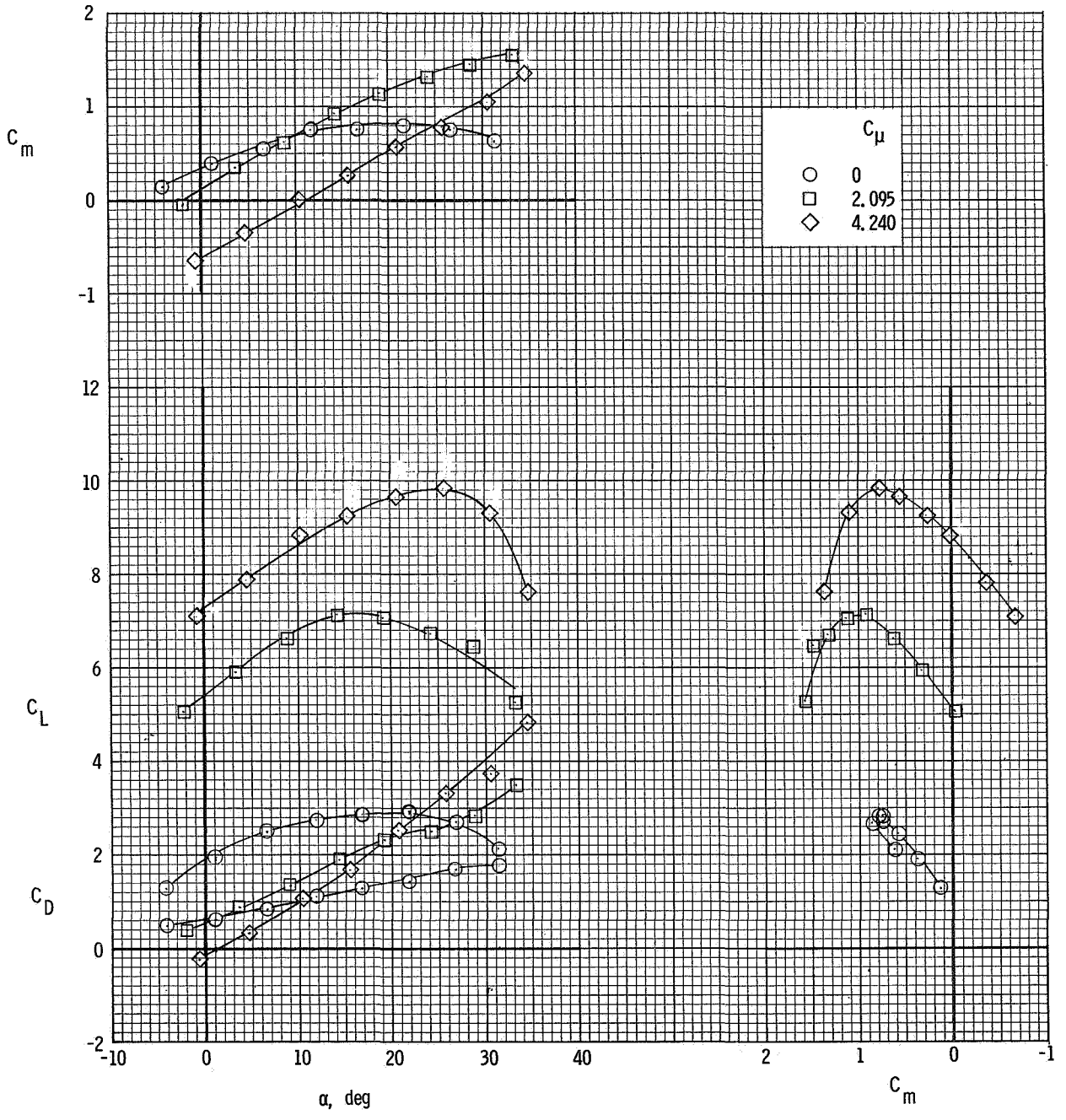

(a) $C_{\mu,BLC} = 0$.

Figure 10.- Longitudinal characteristics of the model with deflector configuration C (see fig. 4(a)). Landing flap configuration $(\delta_f = 60^o, 50^o, 30^o)$.

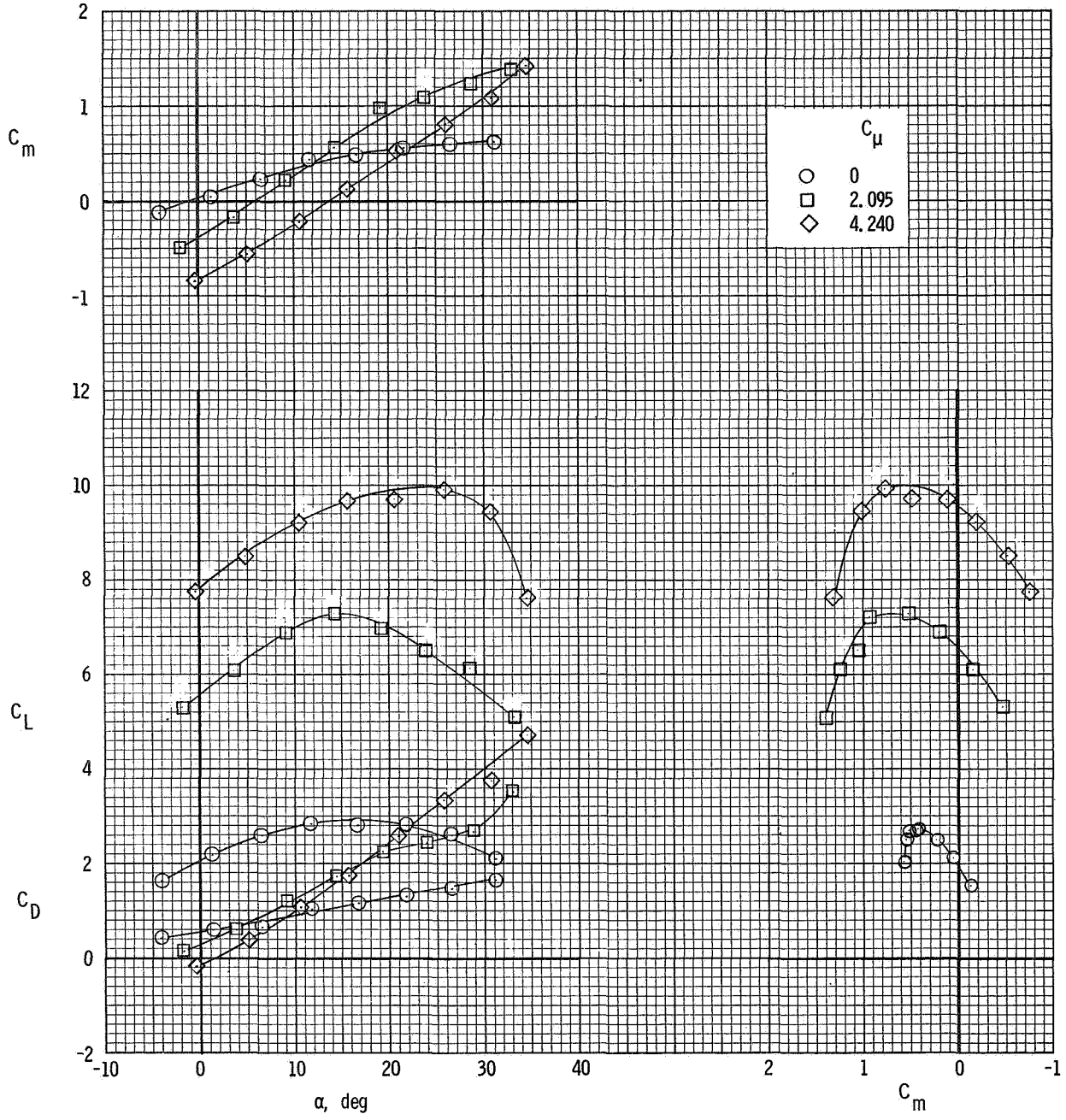

(b) $C_{\mu,BLC} = 0.061$ (outer span only).

Figure 10.- Continued.

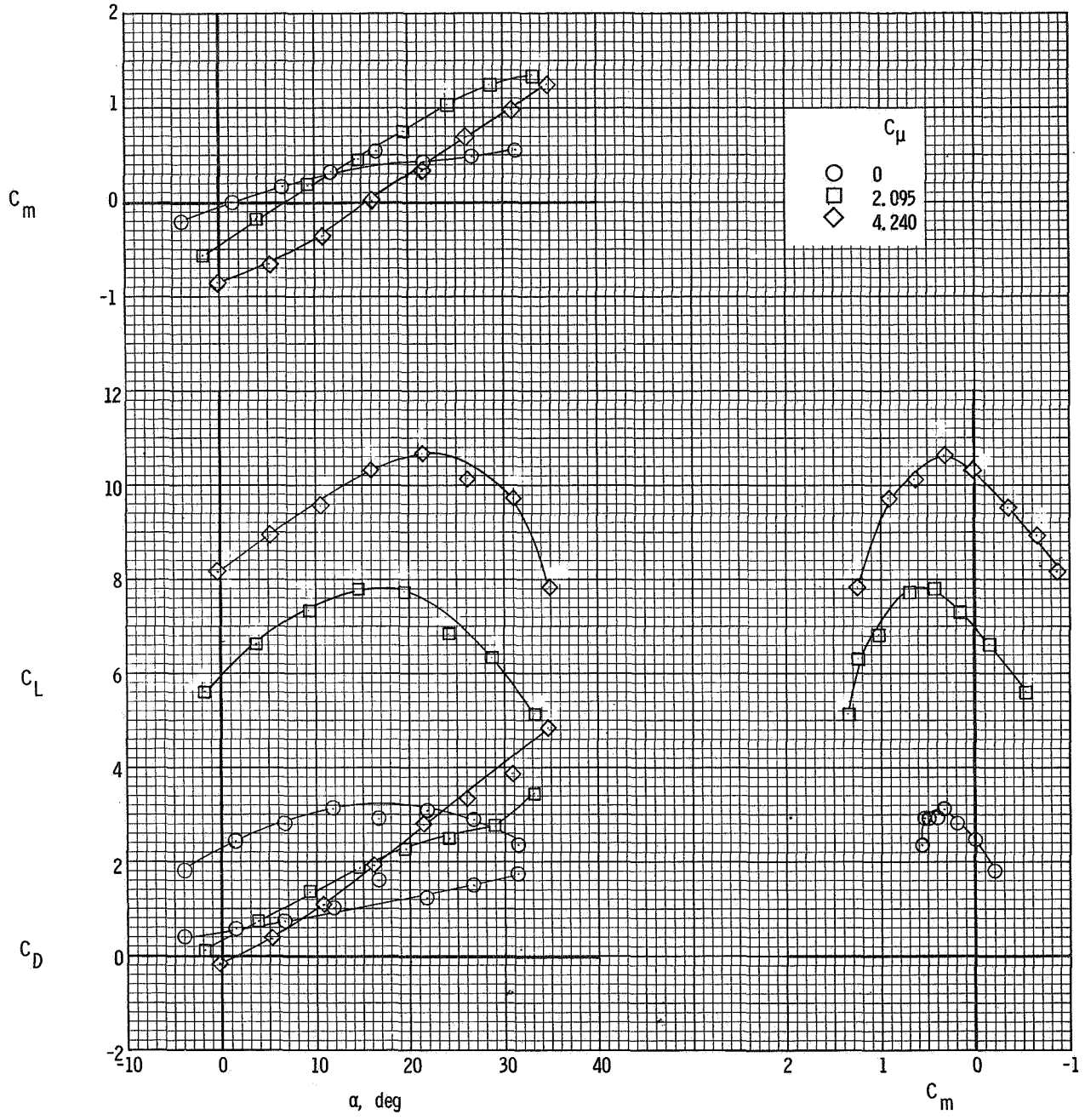

(c) $C_{\mu,BLC} = 0.142$ (outer span only).

Figure 10.- Concluded.

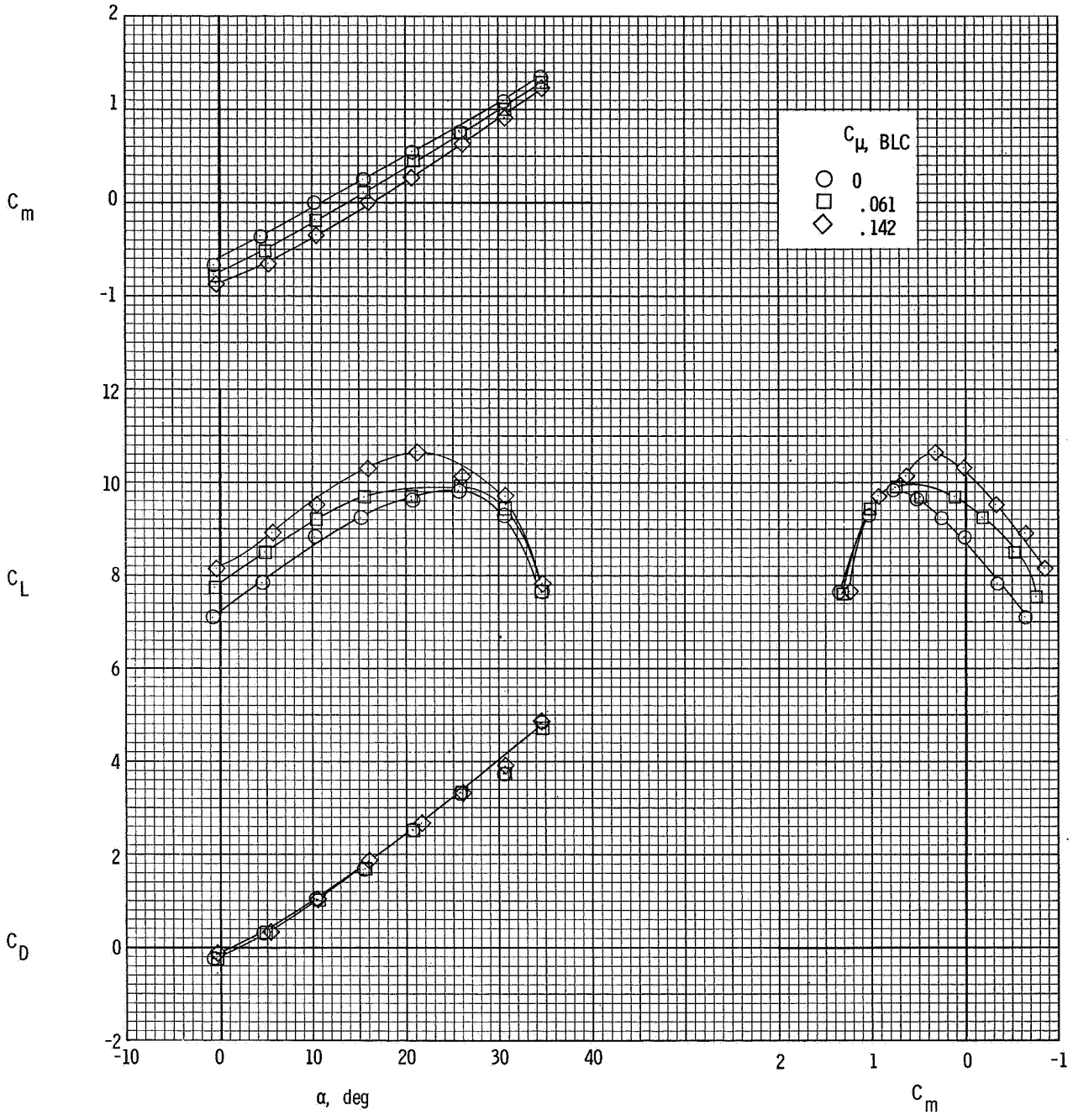

Figure 11.- Effect of blowing boundary-layer control on the lift characteristics of the model with deflector configuration C (see fig. 4(a)). Landing flap configuration $(\delta_f = 60^o, 50^o, 30^o)$; $C_\mu = 4.24$.

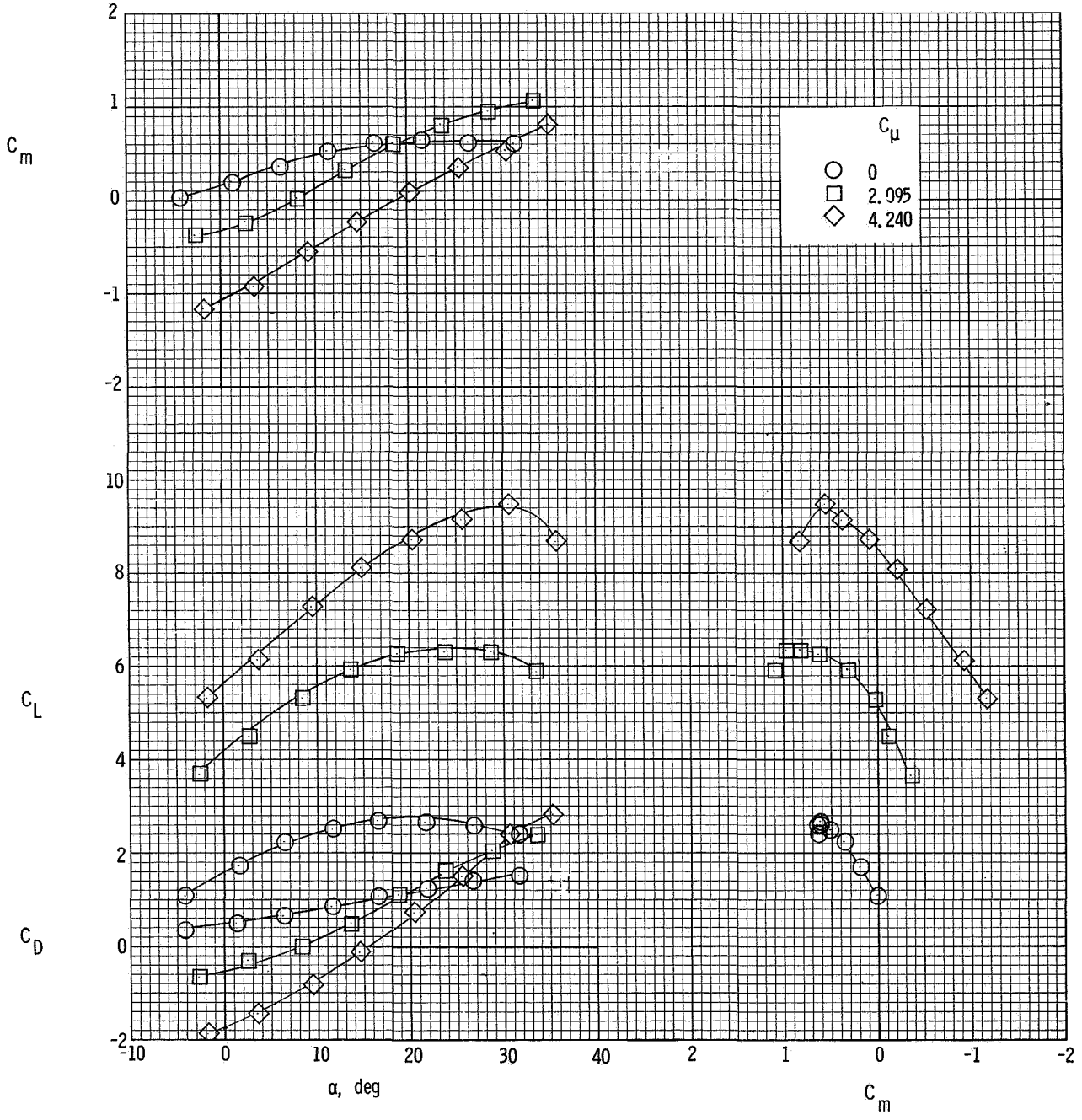

(a) $C_{\mu,BLC} = 0$.

Figure 12.- Longitudinal characteristics of the model with deflector configuration C (see fig. 4(a)). Take-off flap configuration $(\delta_f = 30^o, 30^o, 30^o)$.

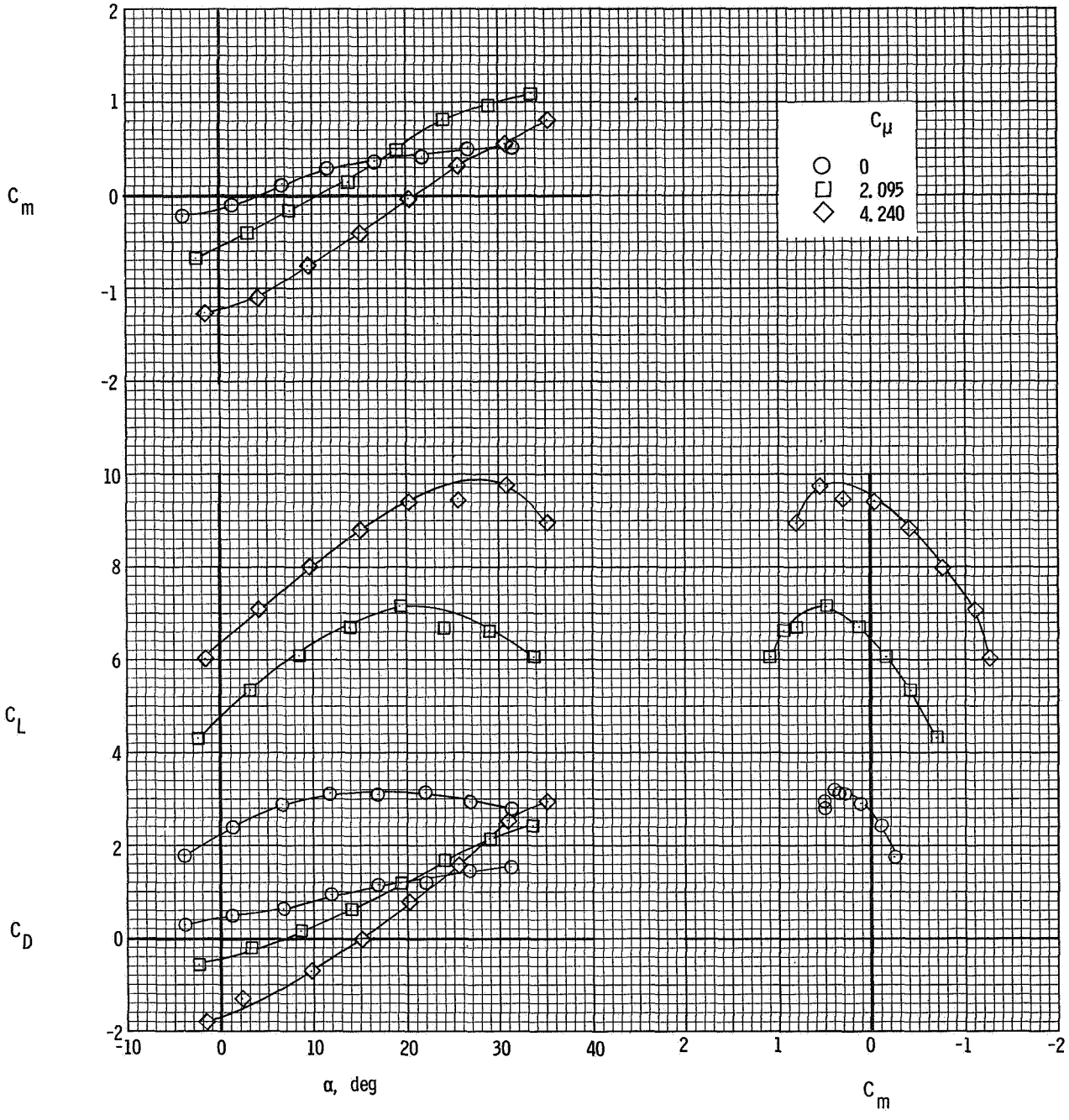

(b) $C_{\mu,BLC} = 0.061$ (outer span only).

Figure 12.- Continued.

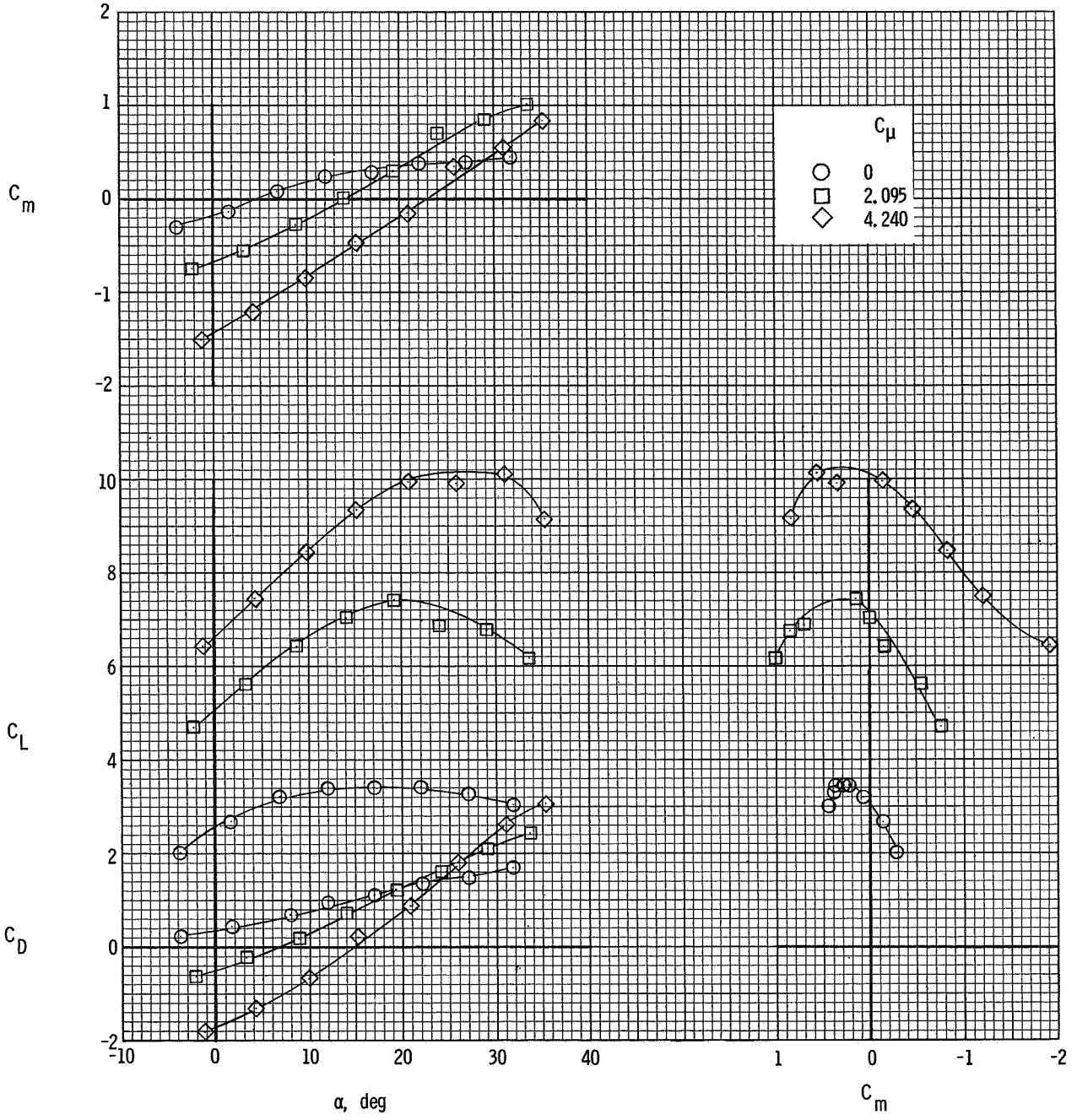

(c) $C_{\mu,BLC} = 0.142$ (outer span only).

Figure 12.- Concluded.

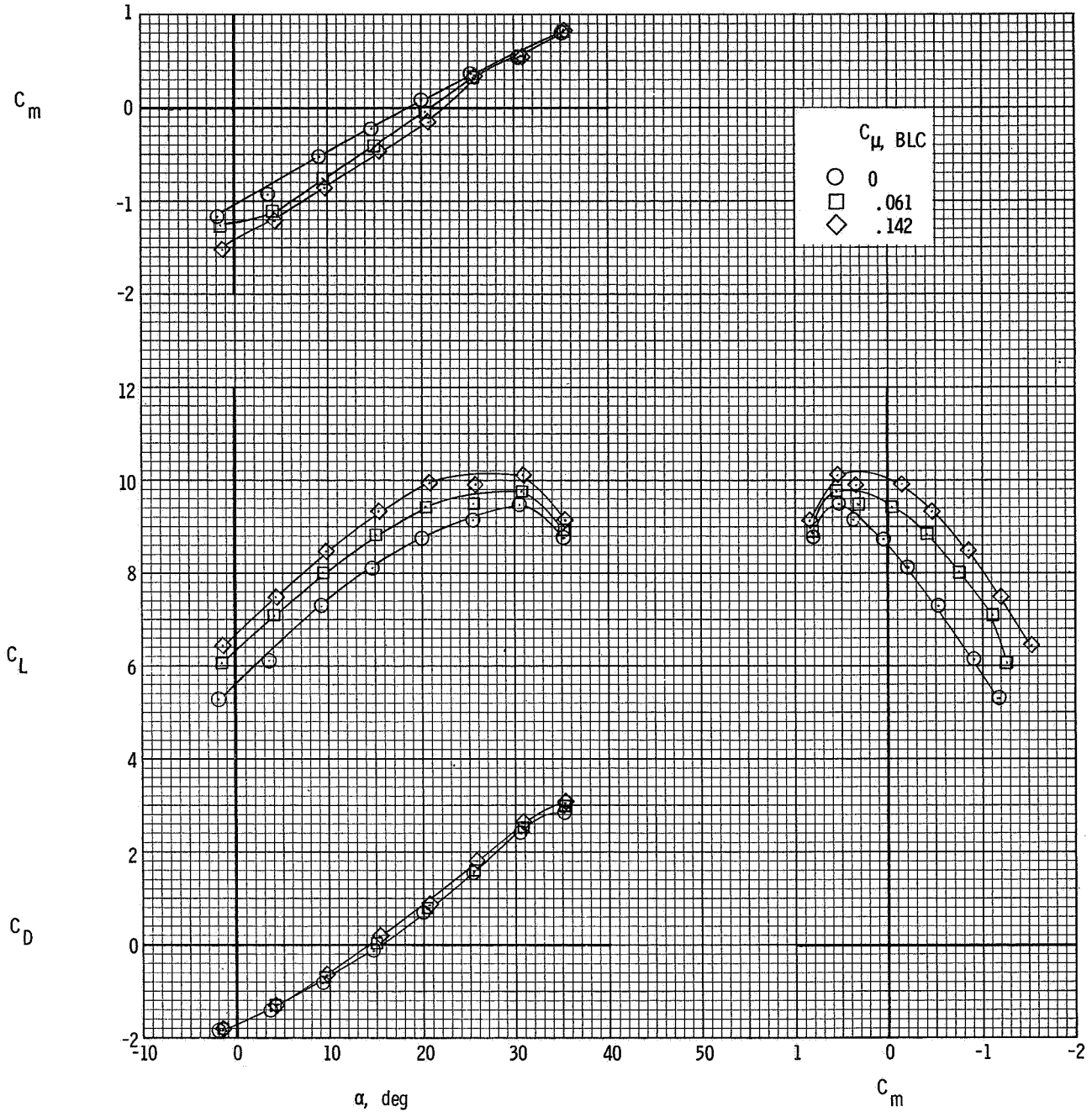

Figure 13.- Effect of blowing boundary-layer control on the lift characteristics of the model with deflector configuration C (see fig. 4(a)). Take-off flap configuration ($\delta_f = 30^o, 30^o, 30^o$); $C_\mu = 4.24$.

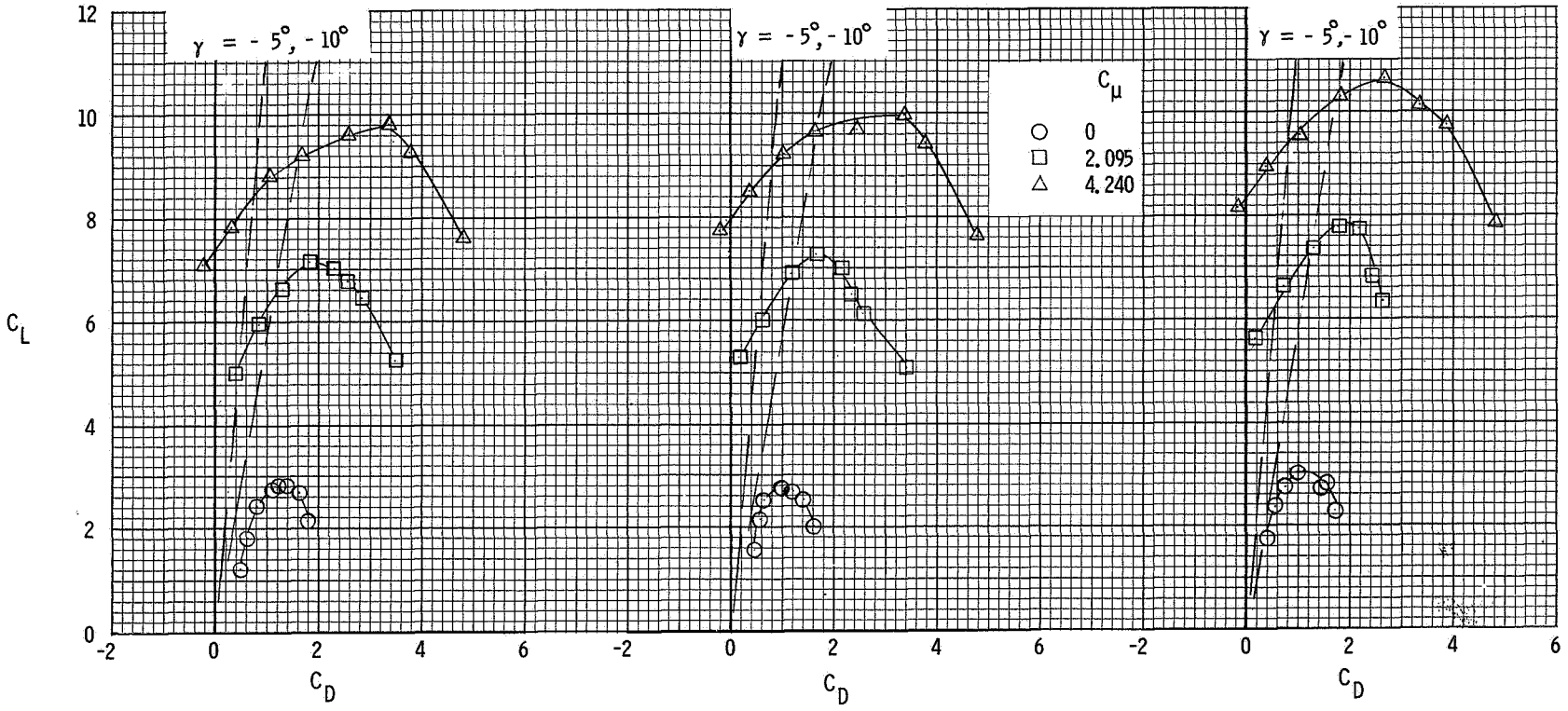

(a) $C_{\mu,BLC} = 0$.

(b) $C_{\mu,BLC} = 0.061$ (outer span only).

(c) $C_{\mu,BLC} = 0.142$ (outer span only).

Figure 14.- Lift-drag polars of model with deflector configuration C (see fig. 4(a)). Landing flap configuration $(\delta_f = 60^o, 50^o, 30^o)$.

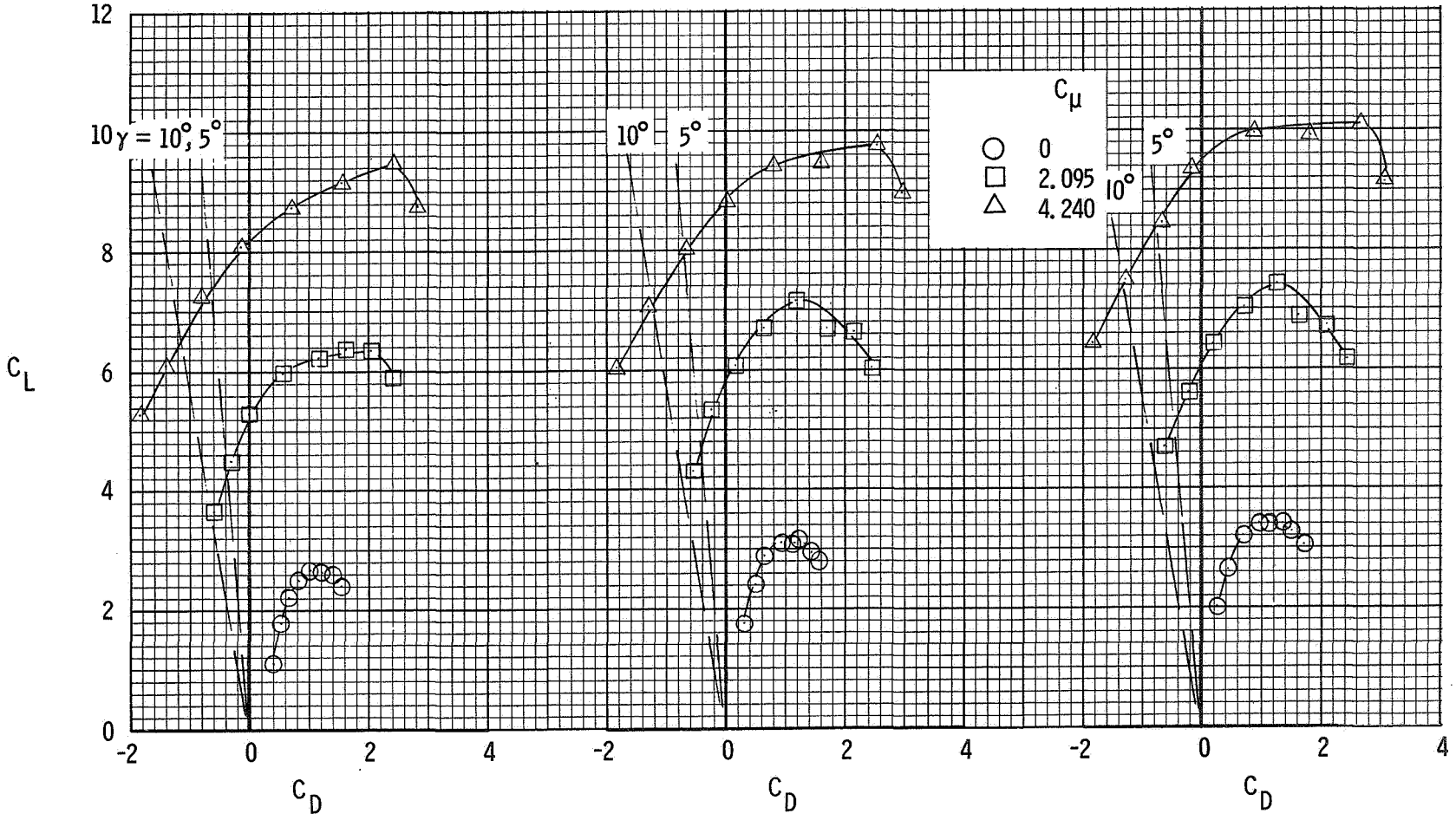

(a) $C_{\mu,BLC} = 0$.

(b) $C_{\mu,BLC} = 0.061$ (outer span only).

(c) $C_{\mu,BLC} = 0.142$ (outer span only).

Figure 15.- Lift-drag polars of model with deflector configuration C (see fig. 4(a)). Take-off flap configuration $(\delta_f = 30^o, 30^o, 30^o)$.

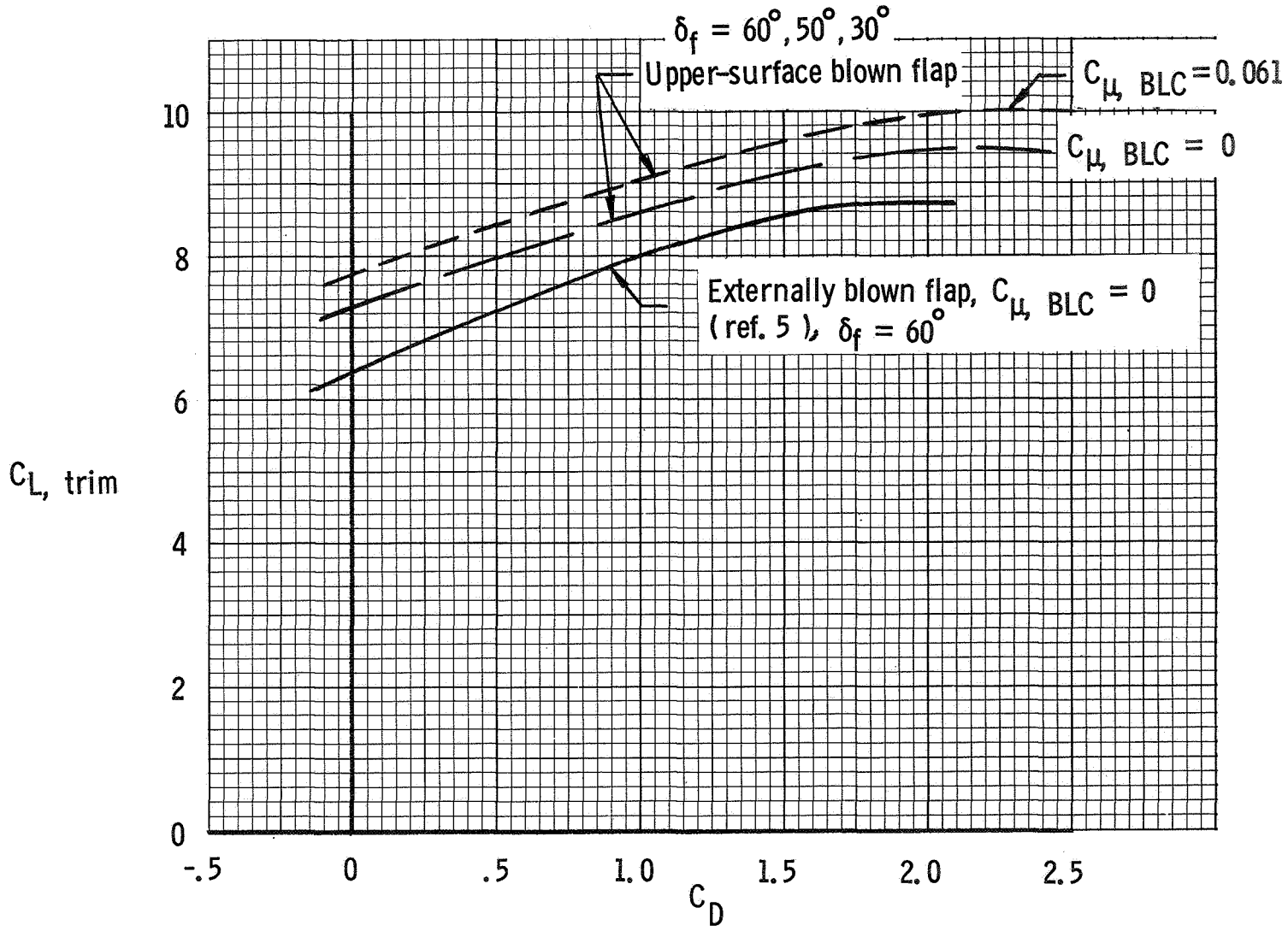

Figure 16.- Comparison of lift-drag polars for USB and EFB concepts. C_μ = 4.24; c.g. = 0.5$\bar{c}$.

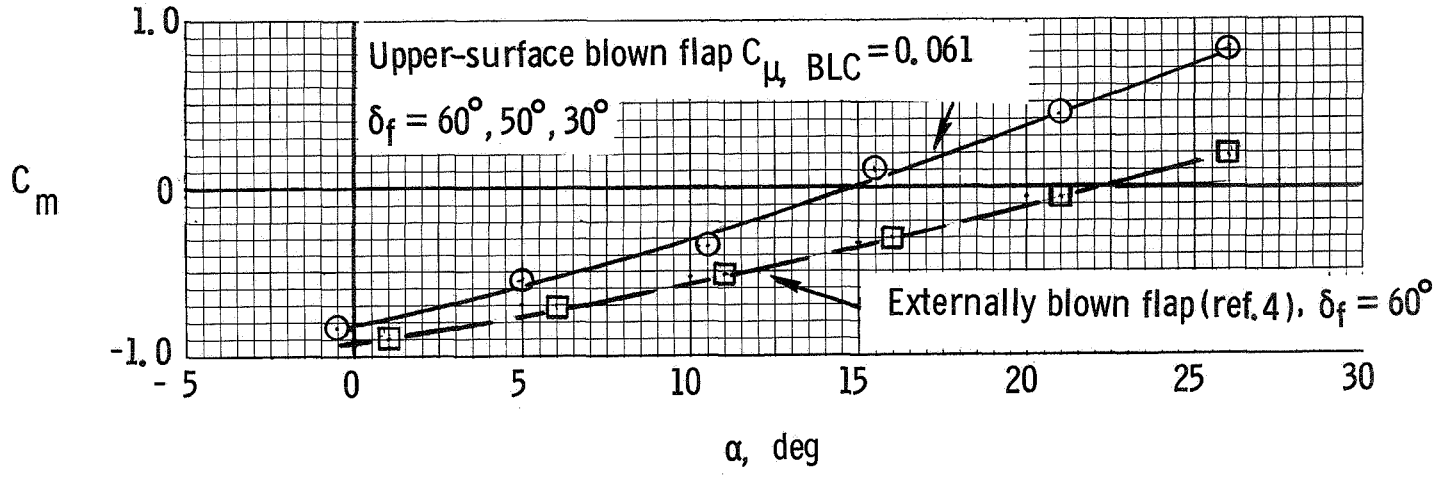

Figure 17.- Comparison of pitching-moment characteristics for USB and EBF concepts. $C_\mu = 4.24$; c.g. = $0.5\bar{c}$.

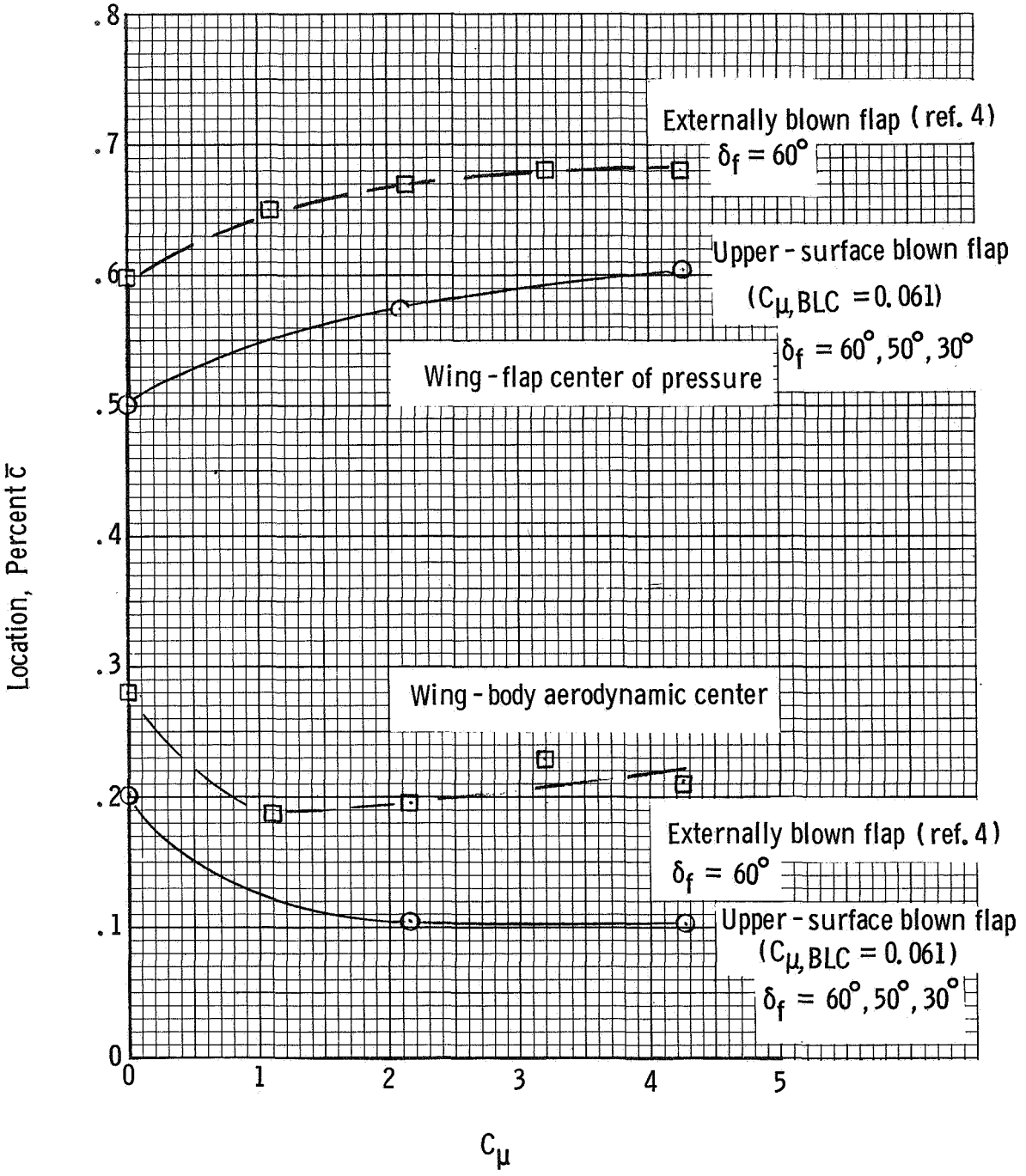

Figure 18.- Variation of locations of wing-flap center of pressure and wing-body aerodynamic center with thrust coefficient. $\alpha = 5^o$.

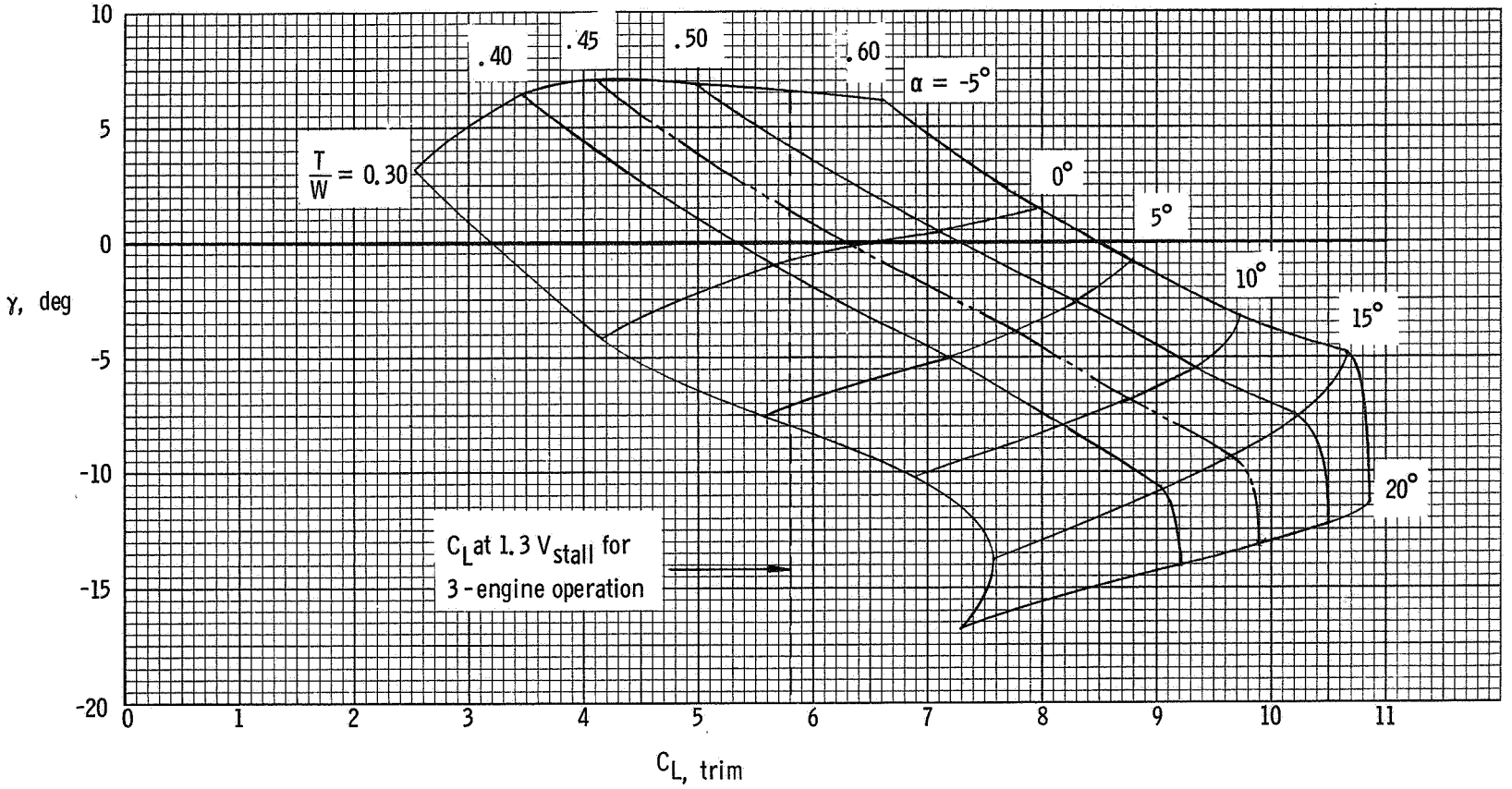

Figure 19.- Flight envelopes for the model. Landing flap configuration $(\delta_f = 60^o, 50^o, 30^o)$; $C_{\mu,BLC} = 0.061$.

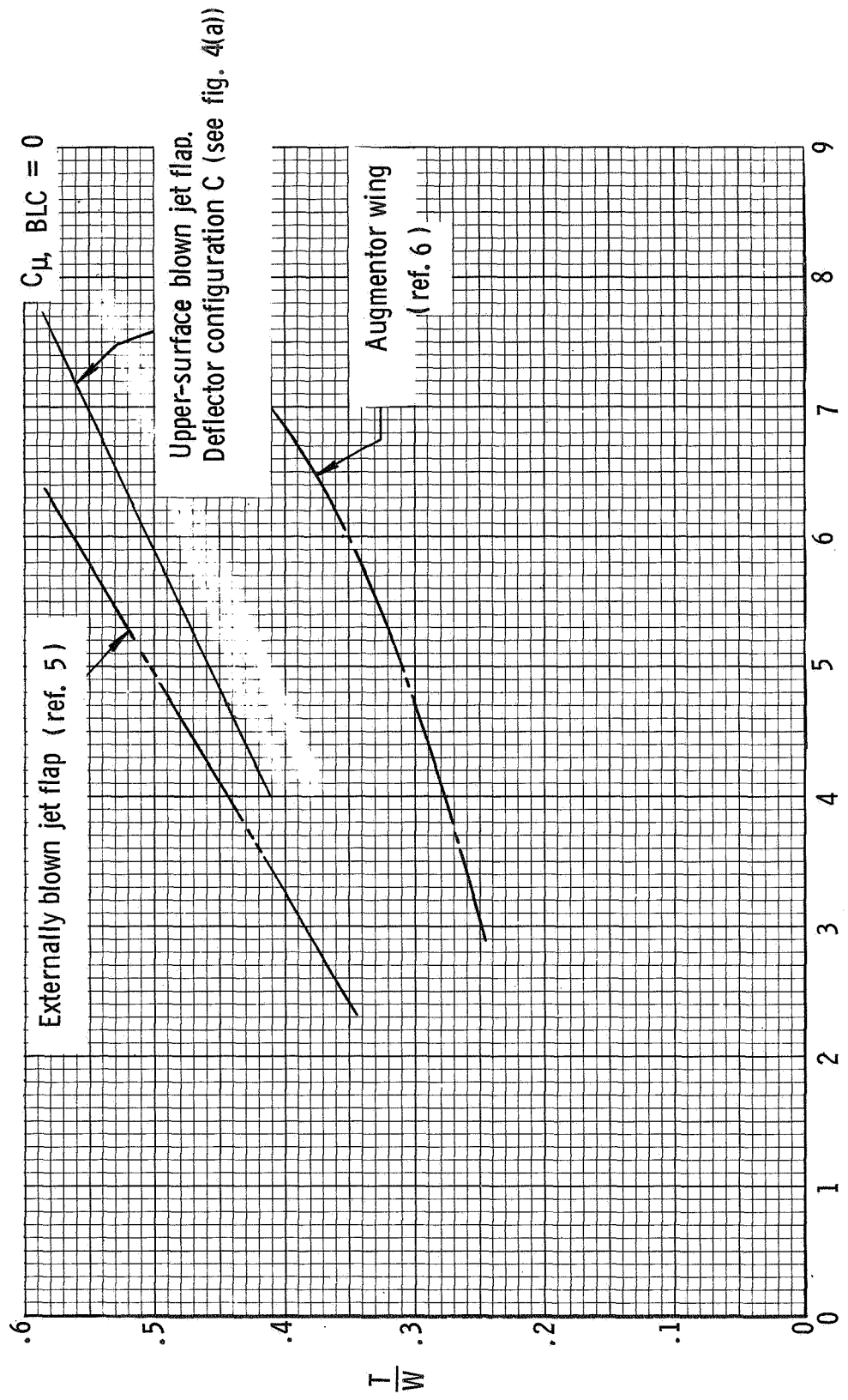

Figure 20.- Thrust-weight ratio required in level flight near $\alpha = 0^{o}$ for several high-lift concepts.

NATIONAL AERONAUTICS AND SPACE ADMINISTRATION
WASHINGTON, D.C. 20546

OFFICIAL BUSINESS
PENALTY FOR PRIVATE USE $300

SPECIAL FOURTH-CLASS RATE
BOOK

POSTAGE AND FEES PAID
NATIONAL AERONAUTICS AND
SPACE ADMINISTRATION
451

U.S.MAIL

POSTMASTER: If Undeliverable (Section 158 Postal Manual) Do Not Return

"The aeronautical and space activities of the United States shall be conducted so as to contribute . . . to the expansion of human knowledge of phenomena in the atmosphere and space. The Administration shall provide for the widest practicable and appropriate dissemination of information concerning its activities and the results thereof."

—NATIONAL AERONAUTICS AND SPACE ACT OF 1958

NASA SCIENTIFIC AND TECHNICAL PUBLICATIONS

TECHNICAL REPORTS: Scientific and technical information considered important, complete, and a lasting contribution to existing knowledge.

TECHNICAL NOTES: Information less broad in scope but nevertheless of importance as a contribution to existing knowledge.

TECHNICAL MEMORANDUMS: Information receiving limited distribution because of preliminary data, security classification, or other reasons. Also includes conference proceedings with either limited or unlimited distribution.

CONTRACTOR REPORTS: Scientific and technical information generated under a NASA contract or grant and considered an important contribution to existing knowledge.

TECHNICAL TRANSLATIONS: Information published in a foreign language considered to merit NASA distribution in English.

SPECIAL PUBLICATIONS: Information derived from or of value to NASA activities. Publications include final reports of major projects, monographs, data compilations, handbooks, sourcebooks, and special bibliographies.

TECHNOLOGY UTILIZATION PUBLICATIONS: Information on technology used by NASA that may be of particular interest in commercial and other non-aerospace applications. Publications include Tech Briefs, Technology Utilization Reports and Technology Surveys.

Details on the availability of these publications may be obtained from:

SCIENTIFIC AND TECHNICAL INFORMATION OFFICE

NATIONAL AERONAUTICS AND SPACE ADMINISTRATION

Washington, D.C. 20546